UNCLASSIFIED

AD NUMBER

AD854149

NEW LIMITATION CHANGE

TO

Approved for public release, distribution unlimited

FROM

Distribution authorized to U.S. Gov't. agencies and their contractors; Administrative/Operational Use; MAY 1969. Other requests shall be referred to Naval Air Systems Command, Washington, DC.

AUTHORITY

USNASC ltr, 26 Oct 1971

THIS PAGE IS UNCLASSIFIED

UNCLASSIFIED

DEVELOPMENT OF CARBON-FILAMENT-REINFORCED METALS

AD854149

Final Report
May, 1969
For the Period 1 May 1968 to 30 April 1969

by

Charles W. Kistler, Jr., and Dale E. Niesz

Prepared under Contract N00019-68-C-0176 for the U. S. Naval Air Systems Command, Department of the Navy, by Battelle Memorial Institute, Columbus Laboratories, 505 King Avenue, Columbus, Ohio 43201.

JUN 24 1969

Qualified requesters may obtain copies of this report direct from the Defense Documentation Center, Cameron Station, Alexandria, Virginia.

[redacted]

THIS DOCUMENT IS SUBJECT TO SPECIAL EXPORT CONTROLS AND EACH TRANSMITTAL TO FOREIGN GOVERNMENTS OR FOREIGN NATIONALS MAY BE MADE ONLY WITH THE PRIOR APPROVAL OF COMMANDER, NAVAL AIR SYSTEMS COMMAND, AIR ____, WASHINGTON, D.C. 20360
520318

UNCLASSIFIED

UNCLASSIFIED

DEVELOPMENT OF CARBON-FILAMENT-REINFORCED METALS

Final Report
May, 1969
For the Period 1 May 1968 to 30 April 1969

by

Charles W. Kistler, Jr. and Dale E. Niesz

Prepared under Contract N00019-68-C-0176 for the U. S. Naval Air Systems Command, Department of the Navy, by Battelle Memorial Institute, Columbus Laboratories, 505 King Avenue, Columbus, Ohio 43201.

Qualified requesters may obtain copies of this report direct from the Defense Documentation Center, Cameron Station, Alexandria, Virginia.

[redacted]

THIS DOCUMENT IS SUBJECT TO SPECIAL EXPORT CONTROLS AND EACH TRANSMITTAL TO FOREIGN GOVERNMENTS OR FOREIGN NATIONALS MAY BE MADE ONLY WITH THE PRIOR APPROVAL OF COMMANDER, NAVAL AIR SYSTEMS COMMAND, AIR_____ WASHINGTON, D. C. 20360

UNCLASSIFIED

FOREWORD

This report was prepared by C. W. Kistler and D. E. Niesz of the Ceramic Research Division, Materials Engineering Department, Columbus Laboratories, Battelle Memorial Institute, 505 King Avenue, Columbus, Ohio 43201 for the U. S. Naval Air Systems Command.

The research program described in this report was performed for the U. S. Naval Air Systems Command under Contract Number N00019-68-C-0176. Mr. M. J. Snyder, Chief, Ceramic Research Division, supervised the work, with Dr. Dale E. Niesz acting as principal investigator and Mr. Charles Kistler, Jr., as project engineer. Mr. J. Lombard supervised the mechanical-property measurements. Much of the filament-coating and sample-layup work was performed by Mr. E. P. Esson.

The work was administered by the Engineering Division - Materials and Processes Branch of the U. S. Naval Air Systems Command (P. R. 9-8-508-07) with Mr. Irving Machlin, Code AIR-52031B, acting as project monitor. The Research and Development Project Number was WF 020-04-01.

This report covers work conducted from 1 May 1968 to 30 April 1969. The work was a continuation of the work performed under Contract Number NOw-65-0615-C and N00019-67-C-0342.

The author wishes to thank Mr. Irving Machlin for his interest and active participation in the program.

ABSTRACT

An investigation was conducted to develop and evaluate carbon-filament-reinforced nickel for use at elevated temperatures. Some effort was also directed toward developing a technique for coating carbon yarns with aluminum, but aluminum-matrix composites were not fabricated.

Dense nickel-matrix composites were fabricated by precompacting and hot isostatically pressing aligned bundles of filaments to which the nickel matrix had been applied as uniform coatings on the individual filaments by electroless deposition. The specimens had uniform microstructures, essentially continuous filaments, and a relatively high-purity phosphorus-free matrix. A significant increase in filament breakage and decrease in composite density were noted when uniaxial rather than radial compaction was used during final densification. Porosity formation and associated microstructural degradation was shown to be dependent on oxygen, nitrogen, and hydrogen impurities in the composite. A vacuum annealing treatment was developed which reduced these impurities to a point where microstructural degradation during high-temperature annealing was insignificant. Removal of these impurities also substantially reduced internal oxidation caused by porosity formation.

The room-temperature tensile strength parallel with the filament orientation was 79,000, 97,000, and 86,000 psi for filament loadings of 43, 49, and 57 volume percent, respectively. Annealing for 100 hours at temperatures up to 2200 F did not reduce the room-temperature strength significantly. However, thermal cycling did produce a significant strength reduction. After 100 cycles to 1800 F, the strength was 58,000 psi, but this strength reduction may be a strong function of the oxygen partial pressure in the atmosphere surrounding the specimen. The strength measured at elevated temperatures decreased more rapidly with temperature than predicted by the simple rule of mixtures. At 2000 F, the measured strength was 36,000 psi.

Possible reasons for the low measured strengths at elevated temperatures are discussed. The reasons for the low strengths (and moduli) measured at room temperature are discussed, and the possible mechanisms for strength reduction due to thermal cycling are reviewed.

The potential of carbon-filament-reinforced nickel is discussed and compared with the experimental data and with the properties of elevated-temperature structural metals. Recommendations are given for further development of carbon-filament-reinforced nickel.

TABLE OF CONTENTS

	Page
INTRODUCTION	1
SUMMARY	3
ALUMINUM COATING STUDIES	4
ANNEALING STUDIES	6
Hydrogen-Methane Atmospheres	6
Vacuum Annealing	7
COMPOSITE FABRICATION STUDIES	8
Uniaxial Hot Pressing	9
Radial Hot Pressing	12
Cold Isostatic Compaction	15
MICROSTRUCTURE AND MICROSTRUCTURAL STABILITY	15
OXIDATION RESISTANCE	20
MECHANICAL-PROPERTY EVALUATION	22
Testing Techniques	23
As-Fabricated Specimens	24
Uniaxially Pressed Plates	25
Radially Pressed Bars	26
Annealed Specimens	31
Thermally Cycled Specimens	32
CONCLUSIONS AND RECOMMENDATIONS	34
TIME EXPENDITURES	36
REFERENCES	37

LIST OF TABLES

Table 1. Gas Content and Weight Change of Nickel-Coated Yarn After Various Annealing Cycles	38
Table 2. Results of Autoclave Run 1	38
Table 3. Results of Autoclave Run 2	39

LIST OF TABLES

		Page
Table 4.	Results of Autoclave Run 3.	39
Table 5.	Summary of Fabrication Parameters, Physical Properties, and Intended Use of Cylindrical Specimens	40
Table 6.	Results of Tensile Tests on Uniaxially Pressed Plate Specimens	41
Table 7.	Results of Interfacial Shear-Strength Evaluations on Uniaxially Pressed Plate Specimens	41
Table 8.	Results of Tensile Tests on Flat Specimens Cut From Radially Pressed Bars	42

LIST OF FIGURES

Figure 1.	Nickel-Coated Yarn After Annealing in Vacuum of 2×10^{-2} Torr at 1830 F	43
Figure 2.	Nickel-Coated Yarn After Annealing in Vacuum of Better Than 5×10^{-3} Torr at 1470 F	43
Figure 3.	Microstructure in Center of Specimen T50-26 Annealed 100 Hours in Argon at 1400 F	44
Figure 4.	Microstructure in Center of Specimen T50-27 Annealed 100 Hours in Argon at 1400 F	44
Figure 5.	Microstructure in Center of Specimen T50-26 Annealed 100 Hours in Argon at 1800 F	45
Figure 6.	Microstructure in Center of Specimen T50-27 Annealed 100 Hours in Argon at 1800 F	45
Figure 7.	Microstructure in Center of Specimen T50-28 Annealed 100 Hours in Argon at 2200 F	46
Figure 8.	Microstructure in Center of Specimen T50-29 Annealed 100 Hours in Argon at 2200 F	46
Figure 9.	Typical Microstructure in Center of Specimen T50-28 Annealed 100 Hours in Argon at 2200 F	47
Figure 10.	Typical Microstructure in Center of Specimen T50-29 Annealed 100 Hours in Argon at 2200 F	47

LIST OF FIGURES
(Continued)

		Page
Figure 11.	Microstructure at Edge of Specimen T50-27 Annealed 10 Hours in Argon at 2200 F.	48
Figure 12.	Microstructure at Edge of Specimen T50-27 Annealed 10 Hours in Argon at 2200 F.	48
Figure 13.	Macrostructure of Nickel Plated Specimen Oxidized 10 Hours in Air at 1400 F	49
Figure 14.	Macrostructure of Nickel Plated Specimen Oxidized 10 Hours in Air at 1800 F	49
Figure 15.	Macrostructure of Specimen T50-28 Oxidized 10 Hours in Air at 1000, 1400, and 1800 F	50
Figure 16.	Macrostructure of Specimen T50-29 Oxidized 10 Hours in Air at 1000, 1400, and 1800 F	51
Figure 17.	Microstructure in Center of Specimen T50-28 Oxidized 10 Hours in Air at 1000 F	52
Figure 18.	Microstructure in Center of Specimen T50-29 Oxidized 10 Hours in Air at 1000 F	52
Figure 19.	Microstructure in Center of Specimen T50-28 Oxidized 10 Hours in Air at 1400 F	53
Figure 20.	Microstructure in Center of Specimen T50-29 Oxidized 10 Hours in Air at 1400 F	53
Figure 21.	Microstructure in Center of Specimen T50-28 Oxidized 10 Hours in Air at 1800 F	54
Figure 22.	Microstructure in Center of Specimen T50-29 Oxidized 10 Hours in Air at 1800 F	54
Figure 23.	Microstructure in Center of Specimen T50-28 Oxidized 10 Hours in Air at 1800 F	55
Figure 24.	Microstructure in Center of Specimen T50-29 Oxidized 10 Hours in Air at 1800 F	55

LIST OF FIGURES
(Continued)

		Page
Figure 25.	Theoretical and Experimental Strength/Density as a Function of Temperature of Carbon-Filament-Reinforced Nickel Compared to Published Data for Various Metals.	56
Figure 26.	Theoretical Elastic Modulus/Density as a Function of Temperature for Carbon-Filament-Reinforced Nickel Compared to Published Data for Selected Metals	57
Figure 27.	Microstructure in Center of Specimen T50-39-3 Cycled 100 Times to 1000 F	58
Figure 28.	Microstructure in Center of Specimen T50-39-1 Cycled 100 Times to 1800 F	58

DEVELOPMENT OF CARBON-FILAMENT-REINFORCED METALS

by

Charles W. Kistler, Jr., and Dale E. Niesz

INTRODUCTION

Recent developments in the production of filamentary materials with high specific strengths and moduli offer a unique approach to developing engineering materials with higher specific mechanical properties. Incorporation of these high-performance filaments in high-temperature oxidation-resistant metal matrices to produce advanced materials is an attractive approach to solving critical materials problems. The temperature range above 1800 F is of particular interest, inasmuch as a variety of applications such as gas turbines, hypersonic airframe structures, and rocket motors could effectively utilize higher specific strengths and moduli than are currently available in nickel- and cobalt-base alloys.

Of the commercially available filaments, carbon shows the most potential for elevated-temperature service in metal matrices. One of the primary reasons for this potential is the thermodynamic compatibility of carbon with nickel and cobalt. Phase diagrams indicate that carbon is stable in cobalt and nickel up to about 2400 F, except for limited solid solubility in each case. This limited solid solubility provides a mechanism for achieving good filament-matrix bonding, which is required in high-performance composites.

On the other hand, the solid solubility may cause microstructural stability problems as a result of carbon diffusion. Also, carbon filaments are not compatible with many oxidation-resistant alloys, since these alloys contain carbide-forming elements. However, aside from aluminum oxide filaments, other available high-performance filaments are not usable in nickel, cobalt, or iron, or their alloys at high temperatures unless suitable barrier coatings are used. Whisker reinforcement also offers an attractive approach to filling many high-temperature materials requirements, but development of the required processing technology and the limited availability of suitable whiskers will combine to produce a longer lead time for these materials than for continuous-filament-reinforced metals.

Carbon filaments are also thermodynamically stable in platinum, copper, and several other metals and show sufficient kinetic stability in several other metals such as aluminum, magnesium, and magnesium-lithium alloys to be of interest for many applications. For some short-time, high-temperature applications, carbon filaments can also be considered for use in conventional superalloys and refractory metals.

The other major reason for the potential of carbon filaments is their current and potential specific mechanical properties. In the current study, filaments were used which had an elastic modulus of 50×10^6 psi, a strength of 295,000 psi, and a density of 1.6 g/cm^3. Filaments are now available which have an elastic modulus of 75×10^6 psi, a strength of 300,000 psi, and a density of 1.8 g/cm^3. Strengths up to 500,000 psi and elastic moduli over 100×10^6 psi have been attained on a laboratory scale with filaments having a density of 2.2 g/cm^3. Although the properties listed above are room-temperature values, the strength and stiffness of carbon filaments should be retained to very high temperatures so that advantageous properties might be obtainable in suitable metal-matrix composites reinforced with carbon filaments.

The research described in this report was a continuation of the developmental effort conducted under Contracts NOw-65-0615-c and N00019-67-C-0342. The overall objective of this research effort was to investigate the potential for carbon-filament-reinforced metals at elevated temperatures, particularly at temperatures above 1800 F.

In the work under Contract NOw-65-0615-c, a fabrication technique was developed which produced carbon filament-nickel composites with uniform filament distributions. This technique consisted of applying uniform nickel or cobalt coatings to carbon filaments by electroless deposition followed by layup, cold rotary swaging and hot isostatic pressing to form dense composites. These composites had low strengths which were attributed to excessive filament breakage during hot isostatic pressing. The phosphorus content of the conventional electroless nickel and cobalt coatings was also undesirable because of matrix embrittlement and eutectic melting well below the melting points of nickel and cobalt.

Under Contract N00019-67-C-0342, the undesirable effects of phosphorus impurities were eliminated through the use of an electroless nickel plating bath which utilized hydrazine rather than sodium hypophosphite as the reducing agent. Furthermore, filament breakage during hot isostatic pressing was essentially eliminated by more parallel alignment in the metal-coated filament bundle. Considerably higher strengths resulted, but microstructural instability (porosity formation) occurred during high-temperature annealing. Poor interfacial bonding and high-temperature-strength data were not obtained because of shear failure in the grip sections of the tensile specimens employed.

The primary objectives of the research described in this report were (1) elimination of porosity formation during high-temperature annealing, (2) elimination of internal oxidation, (3) improvement of interfacial bonding, and (4) measurement of high-temperature strength.

SUMMARY*

Dense carbon-filament-reinforced-nickel composites were fabricated by precompacting and hot isostatically pressing aligned bundles of nickel-coated filaments. Filaments were coated by an electroless deposition technique that yielded phosphorus-free nickel of relatively high purity. This technique gave uniform microstructures and essentially continuous filaments. Some effort was also directed toward obtaining aluminum-coated yarn for composite fabrication.

Annealing studies conducted on nickel-coated yarns showed that the oxygen, nitrogen, and hydrogen contents of the coated yarn could be substantially reduced by heat treating at 800 C in vacuum. Microstructural-stability evaluations confirmed that porosity formation and microstructural degradation during 100-hour anneals at temperatures up to 2200 F could be eliminated by vacuum annealing to remove oxygen, nitrogen, and hydrogen impurities. An additional factor which was found to control microstructural stability during these annealing treatments was the ambient oxygen partial pressure. With low oxygen partial pressures (specimen packed in graphite powder), essentially no microstructural changes occurred during a 100-hour anneal at 2200 F in argon. When specimens were annealed in argon but not packed in carbon, the microstructure near the surface degraded. Specimens showed no strength loss after annealing in argon at 2200 F for 100 hours when packed in carbon. Mechanisms were proposed to explain the effect of oxygen partial pressure and gaseous impurities on microstructural stability.

The oxidation resistance was also found to be improved by removal of gaseous impurities, since internal oxidation caused by porosity formation was nearly eliminated. However, a cladding or an alloy matrix will be required for most elevated-temperature oxidizing environments. The mechanism which leads to this requirement is a microstructural degradation caused by continuous solution of the carbon filaments in the nickel matrix, diffusion of the carbon to the gas interface and removal as CO and/or CO_2. This mechanism causes microstructural changes to a depth of 4 mils after oxidation at 1400 F for 1 hour or 1800 F for 1 hour.

The ultimate tensile strengths and stress-strain behavior of composites were measured on as-fabricated specimens containing 42, 49, and 57 volume percent filaments at room temperature and tensile strengths were measured at 1000, 1400, 1800, 2000, and 2200 F for composites containing approximately 50 percent filaments. The room temperature strength for a 49 percent loading was 97,000 psi, and 79,000 and 86,000 psi for filament loadings of 43 and 57 percent, respectively. The drop in strength on going from 49 to 57 percent loading is attributed to an increase in filament breakage during fabrication. Compared to the strengths predicted from a simple rule-of-mixtures calculation, these strengths were quite low. This fact was attributed primarily to filament breakage and misorientation combined with poor interfacial bonding. For the

*The original data for this research program are contained in Battelle Record Books 25862, 26448, 26824, and 26658.

same reason, elevated-temperature strengths showed considerably more decrease in strength with temperature than predicted by a simple rule-of-mixtures calculation. However, a strength of 36,000 psi was measured at 200 F.

The strengths of specimens after thermal cycling 10 and 100 times to 1000, 1400, and 1800 F were also measured. The results showed that the strength dropped to 58,000 psi after 100 cycles at 1800 F. Based on the results of the annealing studies, however, this strength loss may have been controlled primarily by the partial pressure of oxygen in the atmosphere surrounding the specimen.

The properties of available elevated-temperature structural metals are compared to the theoretical- and experimental-composite properties, and recommendations for further developmental work are given.

ALUMINUM COATING STUDIES

In previous work[1]*, the ability to fabricate carbon-filament-reinforced aluminum by pressure infiltration was demonstrated. However, considerable fiber-to-fiber contact and aluminum carbide formation was noted. One method for eliminating these difficulties is to fabricate specimens by hot pressing of aligned bundles of aluminum-coated yarn. Two coating techniques were evaluated to determine whether an aluminum-matrix composite could be fabricated by this technique. This approach would eliminate carbide formation and should produce more uniform microstructures. Exploratory evaluations were conducted on the adaptability of liquid-phase deposition of aluminum from aluminum diethyl hydride (ADEH) to aluminum coating of carbon yarn. The process involves the decomposition of an aluminum alkyl, aluminum diethyl hydride (ADEH), on heated surfaces of almost any substrate.[2] Decomposition occurs at about 480 F under a protective film of unreacted alkyl which protects both substrate and all coating from oxidation. Since decomposition occurs at surfaces in contact with the solution, uniform coatings can be obtained without a shadowing effect. High plating rates and adaptability to a continuous plating process are other reported advantages of the process. However, the pyrophoric nature of the material requires that the plating solution be protected by an inert atmosphere. Five different techniques for applying these coatings were evaluated, but all were unsuccessful. The primary problems encountered were (1) the high volatility of the solution below the plating temperature, (2) the high surface area of the yarn which leads to rapid heat loss, and (3) the problem of infiltrating a multifilament yarn.

Five pounds of 50 percent ADEH solution obtained from the Continental Oil Company were used to evaluate the feasibility of the liquid-phase-deposition process. The material was shipped under a protective nitrogen atmosphere

*Superscript numbers indicate literature references which are listed at the end of this report.

(15 psig) in a propane tank and was discharged through copper tubing into a glove box containing nitrogen. Although high-purity nitrogen (99.99 percent) was used to purge the glove box, a small amount of "fog" was observed above the ADEH when it was transferred or left uncovered which indicated residual oxygen or moisture was present in the system. Valves installed in the copper-tubing transfer line permitted the line to be cleared of ADEH by flushing with xylene and blowing with nitrogen after each transfer of material to the glove box. Xylene used to flush the tubing was also used to dilute used ADEH to a concentration of less than 25 percent which could be removed from the glove box, exposed to air,[3] and discarded safely.

Several different techniques were evaluated in an attempt to coat single-ply Thornel 50 yarn. In each case, the ADEH was used in the "as received" 50 percent concentration which readily wet the filaments. The first technique consisted of dipping 1-inch lengths of yarn into a test tube containing the ADEH, mounting the saturated yarn on a wire, and pushing the wire into the hot zone of a tube furnace. Rapid vaporization of the ADEH occurred, and coatings were not obtained with furnace temperatures ranging from 480 to 660 F. To overcome the vaporization problem with the furnace heating technique, electrical flash heating of the saturated yarn was attempted. Pieces of single-ply yarn were mounted between duck-bill alligator clips, dipped into the ADEH, and heated electrically with 400 to 1000 milliamperes. Approximately 600 to 700 milliamperes produced a bright orange color. Vaporization was again observed and coatings were not obtained.

The final technique tried in an attempt to deposit coatings involved electrically heating yarn immersed in the ADEH solution. No coatings were obtained when the yarn was preheated with 500 to 1000 milliamperes and dipped into the ADEH for a few seconds. When the yarn was left immersed for several minutes at low current densities (200 to 700 milliamperes), bubbles were released at the yarn, and at higher current densities, the solution quickly boiled over. A heavy granular deposit, which formed around the yarn in a solution of ADEH which had started vaporizing, indicated that heating the ADEH was necessary to initiate decomposition at the heated surfaces of the yarn. Although strip steel and metal parts have been aluminum plated from ADEH solutions, the difficulty encountered with vaporization of heated solutions indicates the process may be difficult to adapt to carbon yarns.

The above experiments to deposit aluminum coatings on carbon filaments were unsuccessful. The high surface area and small diameter of the filaments promoted rapid heat loss from filaments immersed in the ADEH solution, thereby keeping the filament temperature below the minimum 460 F decomposition temperature. Since rapid vaporization of ADEH occurs from a filament heated in the open, deposition on filaments immersed in the ADEH is the more feasible approach. On the basis of these experiments, deposition of aluminum from ADEH is not considered an attractive method of coating the carbon yarns.

Some initial evaluation of chemical vapor deposition from triisobutyl aluminum has also been conducted with moderate success. Lack of uniform plating from filament to filament and granular, somewhat oxidized coatings were the primary problems encountered.

ANNEALING STUDIES

Since dissolution of gaseous impurities was considered the most likely cause of the microstructural instability (bloating) noted in previous work, a vacuum fusion analysis was run on nickel-coated yarn which was typical of that used to fabricate previous test specimens.[4] The analysis showed 1550 ppm oxygen, 125 ppm hydrogen, and 450 ppm nitrogen. Contents of all three elements are quite high, but that for oxygen is particularly high. The hydrogen and nitrogen contents are typical of nickel coatings produced by electroless deposition from a hydrazine bath, but the oxygen content is considerably higher than expected.[5] The high oxygen content probably results from a surface oxidation of coated yarn. Because of the small diameter of the carbon filaments (6.6 microns), the coated yarn has a high surface area, and even a limited surface oxidation would produce a significant oxygen content. In view of these high gas contents, the porosity formation observed in previous work during high-temperature annealing was tentatively attributed to dissolution of these gases and, in the case of oxygen, to an interface reaction with carbon to form carbon monoxide and/or carbon dioxide. Porosity formed by gas evolution could also cause the internal oxidation noted in previous work.[4] In addition, such a gas-forming reaction at the interface could prevent the formation of a good filament-matrix bond. Poor interfacial bonding causes poor transverse tensile strength and reduces the tensile strength parallel with the filament orientation. Technical problems mentioned above could have resulted from the oxygen in the specimens. Therefore, removing the gaseous impurities could improve mechanical properties.

The first step in checking these hypotheses was to conduct an annealing study to determine the feasibility of removing the oxygen, nitrogen, and hydrogen from the coated yarn before specimen fabrication. Samples of nickel-coated yarn were annealed in hydrogen, hydrogen-methane mixtures, and in vacuum and were analyzed for residual oxygen, hydrogen, and nitrogen. All specimens were annealed 1 hour at the maximum temperatures indicated in Table 1.

Hydrogen-Methane Atmospheres

One specimen was annealed in hydrogen at 1700 F by heating and cooling in argon to prevent loss of carbon from the reaction of carbon and hydrogen to form methane. However, a high weight loss of 12.3 percent was encountered which

indicated some carbon had been lost during the run. Metallographic examination indicated that the filaments had been rounded and that the nickel coatings were disrupted. However, the gaseous impurity content was reduced.

Subsequently, specimens were annealed in mixtures of methane and hydrogen with the partial pressure of methane kept at or above the equilibrium pressure for the reaction of carbon and hydrogen to form methane. Weight-change data compiled in Table 1 indicated that nickel-coated yarn annealed in methane-hydrogen at 1110 F did not change weight, whereas yarn annealed at 1300 F and 1470 F gained 0.31 and 10.5 percent, respectively. All of the yarn annealed in methane-hydrogen atmospheres was shiny, and microscopic examinations did not reveal any carbonaceous deposits on the yarn. The gas content of the nickel coated yarn given in Table 1 indicates that annealing in methane-hydrogen at 1470 F was effective in removing the nitrogen, but that the oxygen content remained rather high at 385 ppm. Since oxygen was not removed to a desirable level by annealing in methane-hydrogen atmospheres, effort was directed to an evaluation of vacuum annealing treatments.

Vacuum Annealing

The gas contents reported in Table 1 for nickel-coated carbon yarn vacuum annealed at temperatures from 750 F to 1830 F varied considerably depending on the vacuum obtained during the annealing treatment. Annealings made at an uncontrolled heating rate early in the study resulted in poor vacuums and disruption of the nickel coatings at the higher temperatures. Figure 1 shows filament degradation that occurred during annealing at 1830 F with an uncontrolled heating rate. These filaments also exhibited a weight loss of 0.69 percent compared to only 0.27 percent for yarn annealed in a better vacuum. In addition to the loss of filament and coating integrity, considerable bridging between adjacent filaments has taken place as a result of the sintering. Metallographic examination of filaments vacuum annealed at 1830 F in a good vacuum was not conducted because some filament rounding had already been observed for yarn vacuum annealed at 1470 F in a good vacuum and because the gas content of coated yarn annealed at 1830 F was about the same as that annealed at 1470 F.

Figure 2 illustrates coated yarn which had been vacuum annealed at 1470 F under a controlled heating rate of 400 F per hour in which a vacuum of 5×10^{-3} torr was maintained. Some bridging between adjacent filaments can be seen along with the elimination of sharp irregularities from the surfaces of the filaments. Since coating disruption was negligible and the oxygen content of 240 ppm was not much greater than that for the 1830 F annealing treatment, a vacuum annealing treatment at 1470 F with a heating rate of 400 F per hour was selected as a standard prefabrication treatment throughout the investigation.

The vacuum fusion analysis results presented in Table 1 indicate that gaseous impurities can be partially removed from the coated yarn by suitable

vacuum annealing procedures. In addition, vacuum annealing was considered to be the most effective means of removing gaseous impurities from large batches of yarn which were compressed in mild steel cans for subsequent consolidation. Later gas analyses, conducted on densified specimens which were vacuum annealed 1 hour at 400 and 1470 F prior to hot isostatic compaction, indicated the gas content was, respectively, 550 ppm oxygen, 35 ppm hydrogen, and 100 ppm nitrogen, and, 295 ppm oxygen, 30 ppm hydrogen, and 15 ppm nitrogen. These results were consistent with those reported in Table 1 and demonstrated that large batches of nickel-coated yarn can be effectively outgassed. Although an optimum vacuum annealing temperature has not been determined, the present study has indicated that the total oxygen, hydrogen, and nitrogen contents can be reduced from over 2000 ppm in the coated yarn to approximately 300 ppm and lower by vacuum annealing treatments. This reduction in gas content was expected to reduce porosity formation and improve the interfacial bond strength of composites fabricated from the nickel-coated yarn.

Much of the filament rounding shown in Figures 1 and 2 was attributed to reaction of the filaments with residual oxygen in the vacuum annealing atmospheres. Similar filament rounding was subsequently observed in dense specimens annealed in argon when a low oxygen partial pressure was not maintained in the furnace atmosphere. Because loose filaments were used in the above annealing studies, the partial pressure of oxygen in the furnace atmosphere would be more important than for a bundle of filaments contained in a mild steel can. The importance of maintaining a good vacuum with a low oxygen pressure to prevent carbon loss and filament rounding due to reaction between carbon and oxygen to form CO and to prevent oxidation of the nickel during the heating and cooling cycles is discussed further in the microstructural stability section of this report.

COMPOSITE FABRICATION STUDIES

The technique developed in previous work for fabricating specimens of unidirectionally reinforced composites yielded dense composites with uniform microstructures and essentially continuous filaments.[4] This technique employed nickel-coated carbon filaments as the basic element from which dense composites were formed by a combination of cold compaction and hot isostatic pressing. The essential steps in the technique were as follows:

(1) Separate the two plies of the carbon yarn and remove the residual twist from each ply

(2) Coat the yarn with relatively high purity electroless nickel[4,5] while holding it straight

(3) Separate the layer of coated yarn into segments and layup the segments as layers to form an aligned bundle

(4) Precompact the aligned bundle (density and technique depends on configuration)

(5) Vacuum outgas at 400 F

(6) Hot isostatically press to complete densification.

The details of this technique were described previously.[4]

One difficulty encountered with specimens fabricated by this technique was gross porosity formation (bloating) during high-temperature annealing. The vacuum fusion analyses and annealing studies, discussed previously, indicated that the porosity formation was probably due to the oxygen, nitrogen, and hydrogen impurities in the specimens and that these impurities could be essentially eliminated by vacuum annealing the nickel-coated carbon yarn. Therefore, specimens were fabricated in the present study to investigate the hypothesis that removal of these gaseous impurities would eliminate porosity formation during high-temperature annealing.

Another major objective of this investigation was to measure high-temperature strength. Previous results showed that cylindrical tensile specimens of the geometry used previously were unsatisfactory for these measurements.[4] Therefore, effort during the present program was directed toward fabrication of sheet specimens rather than bar specimens. In thin sheet specimens, the distance over which load would have to be transferred by interfacial shear forces to reach the innermost fibers could be reduced. Thus, the stress gradients between the inner and outer fibers as well as the probability of shear failure would be reduced. Initial attempts were made to fabricate sheets of the same thickness as that desired for tensile specimens by one-dimensional compaction. However, difficulties were encountered, and the majority of the specimens used for most of the mechanical-property evaluations were fabricated into bars by radial compaction. The sheet specimens were then cut from these bars. Both types of pressing were conducted in a high-temperature gas autoclave, although some specimens were also fabricated by conventional hot pressing.

A limited effort was also directed toward setting up a continuous electroplating facility for specimen fabrication, but this task was eliminated in order to concentrate on developing a technique for fabricating acceptable sheet specimens for mechanical-property evaluations.

Uniaxial Hot Pressing

In initial attempts to fabricate sheet specimens, rectangular specimens 3-1/2-inches long by 5/8-inches wide by 1/16-inch thick were fabricated to utilize material economically, reduce grinding time in sample preparation, and evaluate the feasibility of uniaxial compaction. Two tensile bars 1/4-inch wide

were to be obtained from each rectangular specimen. It should be noted that although hot isostatic compaction was utilized in the following fabrication studies, compaction was actually uniaxial normal to the specimen thickness because of the thick can walls and bottoms used to prevent warpage. Thus, compaction was essentially that which would be obtained by uniaxial hot pressing.

In order to investigate the effect of annealing on microstructural stability and filament-metal bonding, a series of specimens was fabricated from coated yarn which had been vacuum annealed at 1110, 1470, 1650, and 1830 F in a vacuum of 5×10^{-3} torr. A control specimen was fabricated without any annealing treatment, and two specimens were fabricated from coated yarn that had been vacuum annealed at 1470 and 1650 F.

The previously described procedures were used to obtain nickel-coated yarn for sample fabrication. The coated yarn was laid up in cans of 1020 steel with inside dimensions of 3-1/2 inches long by 5/8 inch wide by 3/16 inch deep. The side walls and bottoms of the cans had a thick cross section to assure straight specimens for mechanical-property measurements. Cover foils (10 mils thick) were placed over the top of the stack of coated yarn, and the stack was compressed until the cover foil contacted the can. The can size was precalculated so that this compaction resulted in a density of 35 to 40 percent of theoretical, which is well below the point at which significant filament breakage occurs but dense enough that a reasonable compaction ratio occurs during subsequent compaction. It should also be pointed out that compaction beyond 50 percent of theoretical requires a considerable force, which thus makes subsequent compaction, clamping, and welding more difficult. The cover foils were then clamped in position, and the specimens were vacuum annealed and the can backfilled with argon until sealed by electron-beam welding under vacuum. The specimens were hot isostatically pressed according to the following schedule: heat to 1470 F under minimal pressure, heat to 1830 F and pressurize to 5000 psi over a 30-minute period, hold at 1830 F and 5000 psi for 1 hour.

Considerable warpage, occurring during the pressing cycle, indicated that a thicker and/or a stronger can was required to attain straight specimens. Also, one specimen did not consolidate because of a faulty weld, and the other specimens developed leaks as a result of the large compaction ratio before full densification was achieved. The bulk density, annealing treatment, and nickel content of the seven specimens pressed in Autoclave Run 1 are given in Table 2. Because of residual porosity in these specimens, annealing studies to determine microstructural stability could not be conducted. However, the tensile strength and shear strength and of several of the specimens were determined and are discussed in a later section of this report.

In Autoclave Run 2, the fabrication technique described above was used, but to eliminate warping, the cans were made of 304 stainless steel with a 7/32-inch-thick bottom rather than mild steel with a 1/16-inch-bottom. In addition, the depth of the cavity was reduced from 3/16 inch to 5/32 inch to increase the green density and lower the compaction ratio during hot isostatic pressing, and the

radius of the internal corners was increased. Both of these modifications were made to reduce the probability of can failure and leakage during hot isostatic pressing. Five-mil-thick pyrolytic graphite foil was placed above and below the coated filaments in the can to facilitate removal of the densified samples. Ten-mil-thick stainless steel lids were electron-beam welded in place after vacuum annealing the specimen at either 400 or 1470 F. The autoclave cycle used to press this second group of specimens was as follows: heat to 1830 F under a nominal pressure of 300 psi, linearly increase pressure to 5000 psi over a 30-minute period, and hold at 1830 F and 5000 psi for 1/2 hour.

No warpage occurred during the second autoclave cycle, but weld failures or lid fractures in all the specimens caused leakage at the edges of the lids. Results of Autoclave Run 2 are given in Table 3. Because of leakage during the autoclave cycle, full densification was not obtained. As a result, no mechanical-property or microstructural-stability tests were conducted on these specimens.

However, the filaments were removed from a 1-inch-long section of specimen T50-HP8 by leaching in 20 percent nitric acid. Approximately 90 percent of the filaments were continuous over the 1-inch length. In contrast, the flat specimens that were fabricated in the first autoclave run showed appreciable filament breakage. These earlier specimens had densities around 90 percent compared to 83 percent for T50-HP8. Therefore, most of the filament breakage seems to occur at densities above 85 percent. Dense specimens with nearly continuous filaments were obtained by a similar pressing schedule and the same pressure in earlier work when specimens were compacted radially.[4] As a result, the differences in filament breakage for specimens compacted unidirectionally and radially is believed to be a result of a basic difference in the mechanics of densification.

The following model can be used to describe the difference. Assume the initial bundle of metal-coated filaments has a bulk density of 10 percent of the theoretical density of the composite and has the filaments in parallel alignment with minor misorientations. To densify this bundle by radial compaction, interpenetration of filaments is not required and minor misorientations tend to be eliminated. However, more extensive deformation of the filament coatings and/or interpenetration of the fibers is required to achieve full densification of the same bundle by unidirectional compaction. As a result, lower pressures are required for densification, and filament breakage is lower for specimens compacted radially.

In order to check this hypothesis, both cylindrical specimens (radial compaction) and flat specimens (uniaxial compaction) were fabricated in the third Autoclave Run 3. Two flat samples were fabricated and canned as described for Samples T50-HP8 through T50-HP17, except that a 20-mil thick stainless steel lid was used, and the can wall was made slightly wider to facilitate welding. In addition, four cylindrical samples were fabricated as described in previous work[4] and designated with code numbers continued from that work, except that

the volume percent nickel was deleted from the code so that straight numerical coding could be used for simplicity. All four cylindrical samples were cold rotary swaged before vacuum annealing and hot isostatic pressing. The cycle for Autoclave Run 3 was the same as described above for Autoclave Run 2, except that pressure and temperature were held for 1 hour instead of 1/2 hour.

Data obtained from specimens compacted in Autoclave Run 3 are shown in Table 4. One of the flat specimens, T50-HP18, exhibited the highest density obtained to date with the flat-can design, but the other specimen was less dense. Lid failure was not encountered with the 20-mil-thick lids used on these specimens, so both specimens were subjected to the complete pressing cycle. In contrast to the flat specimens, the cylindrical specimens showed essentially complete densification. However, appreciable filament breakage occurred in both the flat and the cylindrical specimens. A check of the swaging data revealed that the circular specimens had been cold swaged to approximately 85 percent of theoretical density rather than the target density of 65 to 70 percent. Swaging to this density is known to cause severe filament breakage. However, there is a significant difference in the bulk density attained for the two types of compaction as shown by the data in Table 4.

As a result of the filament breakage encountered, none of the specimens from this run were used for mechanical-property measurements. However, the last two specimens listed in Table 4 were used to determine the effect of vacuum annealing on microstructural stability. Because of the difficulties encountered in obtaining dense flat specimens by uniaxial compaction, all specimens fabricated throughout the rest of the investigation were of cylindrical design such that radial compaction occurred during the hot-isostatic-pressing cycles.

Radial Hot Pressing

As discussed above, dense specimens could not be obtained by uniaxial compaction of the nickel-coated carbon filaments and more filament breakup seemed to occur than with radial compaction. Since nearly theoretical density with little filament breakage was achieved in previous work by hot isostatic compaction of cylindrically shaped specimens canned in mild steel tubes[4], this technique was adopted to fabricate dense specimens for mechanical testing. However, to obtain flat tensile bars from cylindrical specimens, sufficient nickel-coated carbon yarn was used in each specimen to increase the theoretical diameter to approximately 0.28 inches. From specimens of this size, three flat bars 0.20-inches wide and 0.03-inches thick could be obtained from each cylindrical specimens by cutting them longitudinally with a 0.02-inch-thick cutoff wheel and surface grinding to the final dimensions.

The previously described techniques were used to obtain aligned bundles of nickel-coated yarn for compaction into dense specimens. The swaged diameter for a particular density was calculated from the following equation which was reported earlier:[4]

$$D_s = \frac{D_c}{(X\rho)^{1/2}} \quad , \tag{1}$$

in which D_s is the swaged diameter of the composite; D_c is the theoretical diameter; and X_ρ is the fraction of theoretical density desired. The square relationship between density fraction and swaged diameter in the above equation causes slight differences in swaged diameters to produce large changes in density. In order to swage each specimen to similar densities, the swaged diameters had to be closely controlled to some factor of the theoretical diameter.

Previously, theoretical diameters were calculated from the following equation:

$$D_c = \left(\frac{D_f^2 \; 720 \; N}{V_f}\right)^{1/2} \tag{2}$$

in which V_f, the volume fraction of filaments, was erroneously reported as V_m, the matrix volume fraction.[4] Examination of this equation indicated that a large error could be introduced in theoretical diameter calculations if the equivalent filament diameter, D_f, were not accurately known. In addition, the equation required that the number of single plies be known for each specimen. To permit theoretical diameters to be calculated readily and more accurately, another equation was derived for the theoretical diameter of the composite in which the filament volume was calculated on the basis of filament diameter. In addition, the weight of filaments rather than the number of plies was substituted into the equation, which simplified to the following:

$$D_c = \left(\frac{0.0477 \; W_{cf} \; W_f}{L \; V_f}\right)^{1/2} . \tag{3}$$

where D_c is the theoretical diameter in inches, W_{cf} is the weight of coated filament in grams, W_f is the weight fraction of filament, V_f is the volume fraction of filaments, and L is the filament length in inches. By selecting a "standard" theoretical diameter so that canning tubes of the same size could be used, the equation was conveniently rearranged to:

$$W_{cf} = \frac{D_c^2 \; L \; V_f}{0.0477 \quad W_f} \tag{4}$$

from which the amount of coated yarn required to obtain a desired theoretical diameter can be calculated. If a theoretical diameter and length are selected as "standard", then the volume fraction of filaments is the only variable to be determined since W_f is directly related to V_f. A graphical plot of W_{cf} versus V_f for a theoretical diameter of 0.28 inches was used to determine the proper amount of yarn needed for each specimen fabricated.

After cold rotary swaging, one end of the carbon-steel cans was sealed by electron-beam-welding steel plugs inside the end of the can. Two 1/8-inch-thick

plugs were used in each end. The inner plug, which served as a heat sink to minimize filament damage on welding, was tapered at a 45 degree angle on the inner edge to insure that the can did not shear as it deformed around the plug. The outer plug was not tapered but provided the hermetic seal when welded to the can. With one end sealed, the canned specimens were vacuum annealed at 5×10^{-3} torr or better to remove gaseous impurities entrapped in the nickel matrix during plating. After annealing the other end of the can was sealed in a similar manner. Specimens were leak-checked before hot isostatic pressing by subjecting them to a helium pressure of 200 psi for 10 minutes and immediately submerging the specimens in alcohol when the pressure was released. Specimens which leaked were rewelded and leak-checked again. The specimens were then hot isostatically pressed according to the following schedule:

(1) Preheat to 1830 F under a nominal pressure of 300 psi at a linear rate over a 2-hour period

(2) Linearly increase pressure to 5000 psi over a 30-minute period

(3) Hold at 5000 psi and 1830 F for 1 hour

(4) Cool under minimal pressure.

The above schedule was used for Autoclave Run 3 and duplicated for Runs 4 and 5 in which additional specimens were pressed.

Eighteen cylindrical specimens, approximately 0.28 inches in diameter, were fabricated by the above techniques to provide specimens for microstructural, microstructural-stability, oxidation-resistance, and mechanical-property evaluations. Table 5 summarizes the fabrication parameters, physical characteristics, and the major type of evaluation conducted with these specimens. A total of 36 flat tensile bars was obtained from Specimens T50-30 through T50-41 by cutting each one longitudinally into 3 rectangular pieces from which bulk densities were determined before grinding the reduced gage sections into the bars. The tensile-bar configuration is described in the section of this report dealing with mechanical testing.

The anomalously high densities in Table 5 are believed to be the result of inaccurately determining the volume percentage of nickel in the batch of carbon yarn from which the specimen was fabricated. As reported previously, the actual matrix percentage in the composite was within 4 volume percent of the matrix volume calculated from the weight of the coated and uncoated yarn. Since a 2 percent error in volume percentage can change the density percentage by about 3 percent, the density fluctuations evident in Table 5 may be due to this factor. A revised method of calculating the volume percentage of nickel in the coated yarn would be necessary to improve these calculations in future work. Some volume percentages of nickel were measured on dense specimens. In general, the measured nickel percentages were about 3 percent above those calculated from the weight of the nickel-coated yarn and the physical properties of the yarn.

Cold Isostatic Compaction

Cold isostatic compaction of coated filaments was studied to determine the maximum pressure the filaments could be subjected to without filament breakup and to determine if this technique could be used in place of cold rotary swaging to precompact the coated filaments. A cylindrical specimen was laid up and preconsolidated to approximately 35 percent of theoretical density with rubber tubing as described by Niesz.[4] One end of the rubber tubing was tied shut, and a rubber stopper was inserted in the outer end through which a hypodermic needle was inserted to evacuate the specimen. After evacuation, the second end was tied shut, and the rubber-jacketed specimen was isostatically cold pressed to a pressure of 1000 psi and held at pressure about 30 seconds. A 3/4-inch length was cut from the specimen after pressing, and the process was repeated at pressures of 5,000, 25,000, and 100,000 psi. The nickel was leached from the filaments pressed at each pressure and the filaments were examined for breakup. Essentially no breakup occurred at pressures up to 25,000 psi, and only a small percentage of filaments were broken after pressing at 100,000 psi. The results indicate that pressures currently used in hot isostatic compaction are well below those which could cause filament breakup in a well aligned composite pressed isostatically.

After release of the pressure (100,000 psi) the density of the rubber-jacketed filaments was 52 percent of theoretical. A higher density was probably attained at 100,000 psi, but expansion on release of the pressure lowered the density to 52 percent. When the rubber tubing was removed, however, the density decreased because of insufficient filament-filament bonding. Since a green density of 52 percent was readily obtained in this limited study, it should be possible to improve the technique to retain a density of 65 to 70 percent so that the cold-rotary-compaction step in the fabrication process can be eliminated. By using a temporary binder or by freezing the coated filaments under pressure, the bundle of coated filaments could be precompacted to 70 percent of theoretical and inserted into a can. Further compaction by cold rotary swaging would not be necessary, so the specimens could be immediately vacuum annealed, sealed, and hot isostatically pressed. An advantage of cold isostatic compaction compared to cold rotary swaging would be that complex shapes could be fabricated in the same manner as cylindrical bars.

MICROSTRUCTURE AND MICROSTRUCTURAL STABILITY

In previous work, dense specimens annealed for 100 hours at 1400, 1800, and 2200 F in argon were found to exhibit porosity formation which increased with annealing temperature.[4] This phenomena was tentatively attributed to dissolution of gaseous impurities entrapped in the nickel coating which were not removed during the 400 F vacuum annealing treatment used prior to densification. One object of the present investigation was to determine if the microstructural stability

could be improved by removal of these impurities. As discussed in the section dealing with annealing studies, gas analyses by the vacuum fusion technique indicated that gaseous impurities were significantly reduced by vacuum annealing the nickel-coated carbon yarn at 1470 F. To determine if this treatment improved the microstructural stability from that previously reported for a 400 F vacuum annealing, specimens fabricated for microstructural stability evaluations were given prepressing vacuum annealing treatments at both 400 and 1470 F. As indicated in Table 5, specimens T50-26 and T50-27 were used for most of the microstructural stability studies, but portions of specimens T50-28 and T50-29 were used for some of the latter evaluations.

All specimens used in the evaluation of microstructural stability were 3/8-inch-long by 1/4-inch-diameter sections cut from the as-pressed cylindrical specimens. Sections of specimens T50-26 and T50-27 which contained 49 volume percent nickel were annealed 10 hours in flowing argon in alumina boats and examined metallographically. A small amount of porosity was observed in localized areas of the specimens annealed at 1800 and 2200 F, but no significant differences in the microstructures were detected which could be attributed to the different prefabrication vacuum annealing temperatures. However, the 10-hour-argon-annealing studies did indicate that the specimens were reacting with the furnace atmosphere.

Subsequent annealing studies were conducted for 100 hours in argon with the specimens resting on top of high-purity graphite powder to maintain a low partial pressure of oxygen in the atmosphere. Metallographic results of the specimens annealed at 1400, 1800, and 2200 F for 100 hours are shown in Figures 3 through 11. Figures 3 and 4 indicate that very little microstructural change has occurred in either specimen T50-26 or T50-27 as a result of annealing at 1400 F. Both microstructures are somewhat textured because of some nonuniformity in nickel coating thicknesses on the inner and outer fibers in the individual plies of yarn. Misaligned fibers resulting from fraying of the yarn during coating also contribute to the texture. Figures 5 and 6 show that porosity formation has begun to occur in portions of the same specimens after 100 hours at 1800 F in argon. Most of the porosity is concentrated in areas where there is filament-to-filament contact from nonuniform coatings or misaligned filaments. Again there seems to be little difference in the microstructures for specimens which had been outgassed at widely different temperatures. These microstructures are quite similar to those shown in earlier work after equivalent postfabrication argon-annealing treatments at 1400 and 1800 F.

A significant difference in microstructural features can be noted in Figures 7 and 8 for specimens which were given a postfabrication argon anneal at 2200 F for 100 hours. These specimens have much more uniform microstructures than specimens T50-26 and T50-27. This better uniformity results from better uniformity in filament coating and less filament fraying during coating. The important feature to be noted is the large amount of microstructural change which has occurred in specimen T50-28 compared to specimen T50-29. Figures 9 and 10 are higher magnification photomicrographs of typical areas in the centers of

these specimens showing gross filament degradation and porosity in the specimen containing coated yarn that was vacuum annealed at the lower temperature of 400 F before hot pressing. The elimination of surface irregularities from most of the filaments and the formation of necks between adjacent carbon filaments are predominant characteristics of Specimen T50-28 fabricated from nickel-coated yarn which was vacuum annealed at 400 F. These features are nearly absent in the specimen fabricated from nickel-coated yarn which was vacuum annealed at 1470 F. A significant difference in microstructural characteristics was also observed between the central area of Specimen T50-28 (shown in Figure 9) and the outer edge of this specimen which is shown in Figure 11. In sharp contrast to the interior of the sample, the exterior portion has remained microstructurally stable and is very similar to that of Specimen T50-29 containing coated yarn that was vacuum annealed at 1470 F before hot pressing.

In contrast to the specimens annealed at 2200 F for 100 hours, those annealed for 10 hours at 2200 F were badly degraded at the periphery of the specimens. The only difference in the annealing procedure was that the 100-hour specimens were annealed on a high-purity graphite powder* contained in alundum boats whereas the 10-hour specimens were in an alundum combustion boat without graphite. Specimens wrapped in pyrolytic graphite foil also showed a severe surface reaction during a 10-hour anneal at 2200 F in argon.

The difference caused by putting graphite powder around the specimen is believed to be due to the difference in the local oxygen partial pressure for the two setups. When specimens were surrounded by graphite powder, the local oxygen pressure in the furnace would be quite low and would be in equilibrium with solid carbon according to the relation

$$C + 1/2\ O_2 \rightleftharpoons CO \quad . \tag{5}$$

When no graphite powder was placed in the furnace, the partial pressure of oxygen would be well above that described by Equation (5). Thus, ambient oxygen would be expected to react with the carbon in the composite to form CO according to Equation (5). The mechanism for the reaction would be for ambient oxygen to react with the carbon dissolved in the nickel matrix at the specimen surface and release CO. This reaction would cause further solution of carbon filaments to maintain the equilibrium conditions.[6] Carbon solution would deplete the carbon filaments in the surface and would cause filament rounding as a result of preferential solution of the protrusions on the filaments. This reaction would extend to the depth where the local carbon concentration was not depleted by the surface reaction and the carbon-concentration gradient would result. This depth would depend on (1) the rate of carbon removal from the surface, (2) the rate of solution of carbon filaments in the nickel matrix, and (3) the surface area and volume fraction of filaments. Marked evidence of such a reaction is shown in Figure 12 which shows the edge of a specimen annealed 10 hours in argon at 2200 F with no graphite powder. Filament rounding did not occur in the center

*National Carbon number 48 graphite powder.

(not shown) of this specimen, but rounding occurred to a depth of greater than 10 mils. The reaction does not occur when the specimen is surrounded by graphite powder to maintain the local oxygen partial pressure at the equilibrium value described by Equation (5). The absence of such a reaction is shown in Figure 11 which shows the edge of a specimen which was surrounded by carbon powder during annealing for 100 hours in argon at 2200 F.

The porosity formation and bridging shown in Figure 12 is more difficult to explain; however, it seems to be associated with oxygen. One possible mechanism is as follows. Assume the activity of oxygen in the composite is lower than in the furnace atmosphere. This situation could result, since the carbon filaments in the composite would dictate a low oxygen activity. Then under nonequilibrium conditions, an oxygen gradient would be established with the oxygen concentration decreasing within the specimen. This excess oxygen would diffuse to the nickel-carbon interface and react to form CO and cause porosity formation. Surface-energy relationships could then force into contact those filaments which were connected by porosity.

The mechanism for the microstructural degradation shown in Figure 9 is also difficult to explain, but must be associated with the higher gas content of Specimen T50-28 (nickel-coated yarn, vacuum annealed at 400 F) as compared to Specimen T50-29 (nickel-coated yarn, vacuum annealed at 1470 F). The following is offered as a tentative explanation. When an as-fabricated specimen is heated, gaseous impurities are released at the filament-nickel interface. When the gas pressure exceeds the restraining force of the nickel matrix, porosity is formed. Because the yield stress of the nickel is reduced as the temperature is raised, the volume percentage of porosity increases with temperature. A competing mechanism for release of gas pressure is diffusion of the gas out of the specimen. Therefore, the porosity formed also depends on the rate at which the specimen is heated and the distance the gas must diffuse to reach a free surface. Comparison of Figures 9 and 11 illustrates this point. Once porosity is formed, the pore boundary represents a high-energy surface compared to the nickel-graphite interface. Therefore, the system energy can be reduced by elimination of this free surface. This excess surface energy provides the driving force for removal of carbon from solution in the nickel and precipitation on the portions of the pore surface occupied by carbon fibers (no nucleation barrier). Considerable evidence of carbon deposition by this mechanism can be seen in Figure 9.

However, another possible mechanism would exist if the pores contained hydrogen, namely, reaction of hydrogen with dissolved carbon at the boundary of the pore occupied by the matrix to form methane which could thus decompose at the filament surface to form pyrolytic graphite. The hydrogen would be released by this reaction so that a continuous cycle could be set up.

Another microstructural-degradation mechanism is filament-filament contacts in the as-fabricated microstructure. These contacts provide a mechanism for solution of carbon at filament surfaces and precipitation at the negative radius of curvature at the contact point. The lower carbon solubility at the negative

radius of curvature provides the driving force for the reaction. The carbon solution and precipitation process is less noticeable in the dense composites studied. This may be due to a scarcity of filament-filament contacts or to a difference in the kinetics of the two reactions. However, it was noted that misaligned filaments originating from the yarn fraying during nickel coating caused much more rapid degradation of the microstructure at points where badly misaligned fibers occurred.

Some recent results of other investigators show complete recrystallization of the filaments in a carbon-filament-reinforced-nickel composite after annealing for 4 days at 1100 C (2012 F).[7] These results are in marked contrast to the results obtained in this study (see Figure 10). Dissolved gases or excessive filament-filament contact in Jackson's[7] specimens may explain the differences.

Physical measurements were made of each specimen before and after the 100-hour annealing treatments to determine if porosity formation was accompanied by bloating of the specimens. Less than 0.2 percent expansion was recorded longitudinal to the filament axis and less than 1.0 percent expansion was obtained in a transverse direction after 100 hours at 2200 F. Specimen T50-28 expanded about 0.7 percent in a direction transverse to the filament axis while Specimen T50-29 expanded only 0.3 percent in the same direction. These data combined with the microstructural examination would indicate that the higher vacuum annealing temperature used for Specimen T50-29 was effective in reducing bloating during postfabrication annealing treatments. However, transverse dimensional changes of 0.9 percent were recorded on tensile bars T50-34 and T50-35 annealed during the same 100-hour run at 2200 F, indicating that considerable differences exist between specimens fabricated under similar conditions.

An examination of the bulk-density data in Table 5 reveals that the density of Specimen T50-28 was approximately 6 percent less than that of Specimen T50-29. Some of the microstructural differences in the annealed specimens shown in Figures 7 and 8 may be due to initially different densities resulting from the two prefabrication vacuum annealing temperatures utilized. A comparison of the bulk densities of Specimens T50-30 and T50-31 in Table 5 also indicates that a significantly higher density specimen was obtained by annealing at the higher temperature. Metallographic examination of Specimens T50-28 and T50-29 was not conducted for the as-fabricated specimens, but examination of portions of these specimens that had been oxidized 10 hours at 1000 F revealed that, due to incomplete densification, Specimen T50-28 contained residual pores at points equidistant from adjacent filaments. This residual porosity is attributed to residual gas which is trapped in the composite during the pressing cycle. The following discussion substantiates this premise.

A vacuum fusion analysis of residual oxygen, hydrogen, and nitrogen in densified Specimens T50-26, T50-27, T50-30 and T50-31 was conducted to determine the effect of annealing time on gas content. Results indicated that Specimens T50-27 and T50-31 vacuum annealed at 400 F for 1 and 2 hours before pressing had, respectively, 550 and 410 ppm oxygen, 35 and 74 ppm hydrogen, and

100 and 25 ppm nitrogen. Specimens T50-26 and T50-30 annealed at 1470 F had, respectively, 295 and 205 ppm oxygen, 30 and 41 ppm hydrogen, and 15 and 70 70 ppm nitrogen remaining after pressing. These results indicate that the oxygen and hydrogen contents are minimized by vacuum annealing at 1470 F for 2 hours and that some unknown variable is responsible for the erratic nitrogen contents. The most significant aspect of the above data is that the oxygen content of the specimens vacuum annealed at 1470 F is only about half of those annealed at 400 F.

Although the gas content can be significantly reduced by vacuum annealing the coated yarn prior to hot isostatic compaction, the few hundred ppm residual gaseous impurities could have a profound effect on the microstructural characteristics and mechanical properties of the composites. The oxygen, hydrogen, and nitrogen present in Specimen T50-31 was calculated to give 1.47 cm^3 oxygen, 4.27 cm^3 hydrogen, and 0.10 cm^3 of nitrogen per cm^3 of specimen at standard temperature and pressure. Thus, dissolution of the dissolved gas in this sample could result in the release of 5.84 cm^3 of gas at standard conditions of temperature and pressure. Applying the gas laws, this same gas would occupy only 0.075 cm^3 per cm^3 of sample under pressing conditions of 5000 psi and 1830 F. Thus, a specimen could have approximately 7.5 percent porosity (volume occupied by dissolved gases) if all the gas were released. However, some of the gas is present as an oxide phase and/or dissolved in the nickel matrix, making an accurate estimate of the free gas content difficult. If, however, one considers the difference in gas contents between two samples as being representative of the difference in porosity which can develop, this porosity can be calculated. Since Specimen T50-31 contained approximately twice the gas content of T50-30, the difference in the gas content is about equal to the gas content of T50-31, or 0.075 cm^3 of gas per cm^3 of specimen. With a theoretical specimen density of 5.25 grams per cm^3 at a nominal 50 volume percent filament loading, the above dissolved gas would reduce the density to 4.88 grams per cm^3 – about 93 percent of theoretical. Although bulk densities this low were not obtained for hot isostatically pressed cylindrical specimens, the 6 percent difference between the bulk densities of Specimens T50-28 and T50-30, and of T50-29 and T-50-31 in Table 5 may be due to entrapped gases present in the specimens. If the oxygen in the specimens is released predominantly as CO, the volumes used for oxygen in the above calculations should be doubled.

OXIDATION RESISTANCE

In previous work, the poor oxidation resistance of cylindrical specimens after 10 hours at 1400, 1600, and 1800 F was attributed to preferential internal oxidation along the axis of the carbon filaments and/or residual porosity in the as-fabricated specimens.[4] In the present investigation, two methods of improving the oxidation resistance were evaluated. The first involved cladding the ends of the specimens with electroplated nickel to prevent preferential oxidation

along the axis of the filaments. The second and more successful technique was to vacuum anneal the coated yarn before densification to remove entrapped gases. In this study, specimens, vacuum annealed at 1470 F before pressing, were significantly more oxidation resistant than those vacuum annealed at 400 F.

In order to evaluate whether oxidation resistance could be improved by eliminating preferential oxidation along the axis of filaments, cylindrical specimens approximately 1/2-inch long and 3/16-inch diameter were capped on both ends by electroplating nickel from a commercial sulfamate bath. The specimens, prepared under a previous contract, contained 46 volume percent nickel and had been vacuum annealed 1 hour at 400 F before pressing. To insure that the 0.004-inch-thick coating was dense before starting the oxidation run, the plated specimens were heated in argon and sintered at temperature 1 hour before changing to an air atmosphere for an additional 10 hours. Specimens were oxidized in flowing air at 1400, 1600, and 1800 F, after which they were sectioned and examined metallographically.

Figure 13 shows that preferential oxidation along the filament axis was minimized by the coating. Disruption of the coating evident in Figure 13 may be the result of internal gas pressure developed by dissolution of entrapped gases during the 1400 F heat-treatment. A similar phenomena was noted for the specimen oxidized 10 hours at 1600 F. Figure 14 indicates that complete deterioration occurred for the specimen oxidized at 1800 F for 10 hours in flowing air. Similar deterioration was previously reported for uncapped specimens oxidized 10 hours at 1800 F.

The bloating which occurred in the above specimens indicated a gas pressure was developing which could fissure the specimen at 1800 F. Subsequent oxidation tests were conducted on specimens which were fabricated with nickel-coated yarn which had been carefully annealed 2 hours at a vacuum of better than 5×10^{-3} torr before pressing. Specimens T50-28 and T50-29 listed in Table 5 were used for this study. Note the difference in the bulk densities of these specimens. The anomolously high value for T50-29 is believed to be the result of an inaccurate determination of the volume percentage of nickel on the coated yarn, but there does seem to be a definite improvement in density for the specimen annealed at 1470 F compared to the one annealed at 400 F. Sections approximately 3/8-inch long by 3/16-inch diameter cut from these specimens were oxidized under ambient air for 1 hour and 10 hours at temperatures of 1000, 1400, and 1800 F. Specimens were pushed into the hot zone of an open-end furnace when the desired temperature had been reached and pulled from the hot zone to terminate the run. Changes in the diameters and weights of the specimens were obtained before examining them metallographically.

Figures 15 and 16 are 10-power photographs of Specimens T50-28 and T50-29 which had been oxidized 10 hours at 1000, 1400, and 1800 F in static air. Preferential oxidation along the filament axis can be observed at localized areas as fissures in the portions of the specimens mounted with the filament axis parallel with the polished face. These fissures appear as dark spots in those portions

of the specimen mounted with the filament axis perpendicular to the polished face. They are probably caused by a porous area in the specimen. The other macroscopic features which can be noted are that the exposed ends of specimens oxidized at 1800 F are slightly concave and that the portion of Specimen T50-28 oxidized at 1800 F appears rippled in the transverse mount of the specimen.

Higher magnification photos of these specimens, shown in Figures 17 through 24, reveal microscopic features which cannot be detected in the macroscopic photos. Figures 17 and 18 show that internal oxidation has started in Specimen T50-28 but is negligible in T50-29 after 10 hours at 1000 F. A gross change is evident after 10 hours at 1400 F as Figures 19 and 20 indicate. Most of the carbon filaments in Specimen T50-28 have oxidized, but little change has occurred in T50-29. Figures 21 and 22 show that filament rounding has reached the centerplane of Specimen T50-29 whereas no filaments are left in T50-28. Figures 23 and 24 are 500-power photos of the 1800 F specimens which show the porous structure of T50-28 and filament degradation in T50-29. The microstructure at the edges of Specimen T50-29 was observed to be similar to the bulk of T50-28 shown in Figure 23.

The significant difference in oxidation resistance is attributed to different residual gas contents and bulk densities in the two specimens evaluated. Although gas analyses were not obtained for these particular specimens, the oxygen, hydrogen, and nitrogen content of other specimens (T50-30 and T50-31) vacuum annealed for 2 hours at the same temperatures of 1470 and 400 F was, respectively, 205 ppm oxygen, 41 ppm hydrogen, and 70 ppm nitrogen, and 410 ppm oxygen, 74 ppm hydrogen, and 25 ppm nitrogen. As discussed in the microstructural-stability section of this report, the difference in the gas content of these specimens can result in the formation of about 7.5 percent difference in porosity. The difference in oxidation resistance between the above specimens is, therefore, attributed to the porosity formed in Specimen T50-28 on heating which promotes oxidation of the specimen.

The excessive filament rounding shown in Figure 24 is probably caused by the same mechanism that caused filament rounding during annealing at 2200 F in argon with an oxygen partial pressure above that given by Equation (5) (Figure 12). The reaction rate would be accelerated, however, because of the higher oxygen partial pressure in an air atmosphere. No filament rounding was evident after oxidation for 10 hours at 1000 F. After 10 hours at 1400 F or 1 hour at 1800 F, filament rounding was noted at a depth of approximately 4 mils.

MECHANICAL-PROPERTY EVALUATION

Limited mechanical properties of carbon-filament reinforced nickel composites were previously reported by Niesz.[4] In that work the ultimate tensile strengths and elastic moduli obtained at room temperature were less than theoretical and the interfacial bond strength measured perpendicular to the filament

axis was low. Two of the objectives of the present investigation were to improve the interfacial bond strength and to obtain representative elevated-temperature mechanical-property data, since previous specimens sheared from the grips in elevated-temperature tests. In addition, a more intensive evaluation of factors affecting the room-temperature strength were determined. Room-temperature stress-strain data were obtained from as-fabricated, annealed, and thermally cycled tensile bars to determine the effect of postfabrication heat treatments and thermal fatigue on the mechanical properties of the composites. A limited evaluation of interfacial shear strength was conducted, and eight specimens were tested at temperatures up to 2200 F.

Testing Techniques

Flat-sheet test specimens were used exclusively for mechanical-property determinations in the present investigation. Previously, cylindrical-shaped tensile bars were used in which room-temperature failure occurred at the end of the gage section and in which shear failure occurred at elevated temperatures.[4] Consequently, thin-sheet specimens were fabricated to decrease the area over which shear stresses must be transferred to carry the load applied to the specimen. The problem of stress concentrations resulting from a low interfacial-bond strength was discussed in earlier work.

Two sheet tensile specimen designs were utilized in the testing program. Test bars without a reduced gage section were made from porous, unidirectionally reinforced plate specimens to evaluate gripping techniques with serrated, bolt-tighten grips. These test specimens were nominally 3-1/4-inches long by 0.035-inch thick by 0.177-inch wide. Alignment holes 1/16 inch in diameter were placed 1/8 inch from either end by electric discharge machining. The specimen grips were of the type that has one removable face which fastens to the other face with four bolts. Each face had serrations running perpendicular to the tensile axis, and a 1/16-inch-diameter loading pin was provided for pinning the specimen to effect alignment. Specimens were mounted for testing by placing the specimens in the grips with 1/16-inch-diameter pins, preloading to attain alignment, and then tightening the four bolts on each grip to secure the specimen. The pins were removed before testing. Strain was measured with a clip-on extensometer with a 1/2-inch gage length.

The gage section was reduced in all subsequent specimens to conform to the specimen geometry proposed by ASTM Committee D-30.[8] This geometry defines the width of the grip section to be equal to the gage width plus twice the specimen thickness. The geometry of the tensile bars fabricated with a reduced gage section consisted of a 1-inch gage section 0.14-inch wide and 0.03-inch thick sandwiched between 1/4-inch-long tapered sections. The tapered sections met the gage section with a 1/2-inch radius at each end. Grip sections 0.20-inches wide and 3/4-inch long brought the total specimen length to about 3 inches. The specimens were of uniform thickness over the entire length. All specimens were

cut and ground to shape with water-cooled grinding equipment. Alignment holes 1/16 inch in diameter were electric-discharge machined through the specimens 1/8 inch from each end.

A few of the specimens with reduced gage sections were tested at room temperature using 320-mesh emery cloth loading pads in the serrated, bolt-tighten grips described above. Most, however, were tested in self-aligning, self-tightening molybdenum grips (TZM alloy) which consisted of a collar having a wedge-shaped slot in one end and threads for the loading rod in the other. The tensile bars fit inside split TZM wedges, forming an assembly which matched the 10 degree included angle of the slot in the collar. An alignment pin was located in the thick end of each set of wedges to locate the specimen in the center of the grip assembly and to provide for initial specimen loading. Pyrolytic graphite foil was inserted between the outer faces of the wedges and the slots in the collars to facilitate self-tightening of the wedges when a load was applied. However, it was necessary to put a small piece of double-stick transparent tape between the wedges and the graphite foil at the location of the alignment pins to prevent premature gripping of the specimen before a load was applied. As the specimen load was increased the tape was compressed into the graphite foil. providing uniform loading of the specimen over the entire face area of the wedges. The machine finish on the inner faces of the wedges was sufficient to prevent specimen pull-out from these grips so serrated gripping faces were not necessary.

All tests were made in an Instron Testing Machine with a cross-head speed of 0.01 inch per minute. Upper and lower loading rods containing universal joints were used with both the bolt-tighten and self-tightening grip assemblies to reduce bending moments from specimen misalignment. For room-temperature tests a clip-on extensometer with a 1/2-inch gage section was used to obtain strain readings. No strain readings were obtained during elevated-temperature tests which were conducted with a radiant furnace. A forming gas (10 percent hydrogen and 90 percent nitrogen) atmosphere passed through a dense mullite tube surrounding the specimen and grip assembly protected both from oxidation during elevated temperature tests. Because the furnace was heated rapidly to the testing temperature and the specimens were dense, the reaction of hydrogen and carbon to form methane was nominal as confirmed by weight checks on the specimens before and after each test.

As-Fabricated Specimens

Specimens fabricated by uniaxial pressing early in the program were consistently less than theoretical density but were tested at room temperature to evaluate testing techniques and provide some data for comparison with that of radially pressed specimens. Limited shear strength determinations were also made on these porous specimens to determine if vacuum annealing the coated

yarn affected the shear strength. Radially pressed specimens were evaluated on the basis of room temperature and elevated temperature tensile strength but no shear strengths determinations were made on these specimens.

Uniaxially Pressed Plates

Table 6 shows the results of room-temperature tensile tests to evaluate various gripping techniques with the bolt-tighten grips. Emery cloth and aluminum foil loading pads were used to prevent specimen damage from the coarse serrations. The emery cloth was effective in preventing specimen damage, but the aluminum foil was not. However, since gage failure occurred in only two of three specimens, a reduction in the gage section was considered desirable. The low strengths and moduli of the uniaxially-pressed specimens in Table 6 are attributed to residual porosity and filament fractures during fabrication.

A microscopic examination of filaments leached from Specimens T50-HP1 and T50-HP7 indicated that considerably more filament break-up occurred in the specimen vacuum annealed at 1830 F before pressing than in the specimen which received no vacuum annealing treatment. Because both specimens had comparable bulk densities, the difference in filament break-up was attributed to differences in fabrication behavior caused by the two annealing temperatures. Because the autoclave preheat temperature was only 1470 F, filaments in the sample vacuum annealed at 1830 F before pressing were probably sintered together and broken up when pressure was applied at 1470 F. Filaments in the sample prepared from unannealed yarn were not sintered together and were free to conform when pressure was applied. For comparison, filaments leached from Specimen T50-HP18 pressed to 97 percent of theoretical exhibited about the same degree of break-up as those from Specimen T50-HP7 pressed to 93 percent of theoretical. For T50-HP18, the lower 1470 F vacuum annealing temperature combined with the higher preheat temperature of 1830 F used in the autoclave cycle permitted a higher density to be obtained without additional filament break-up.

The larger portion of the above fractured tensile specimens was used for the shear measurements. Three slots were formed near the center of the 0.177-inch-wide specimens perpendicular to the length of the specimen (direction of filament orientation) by electric-discharge machining. A 50-mil-deep slot was formed in each side of the specimen on the same plane, which reduced the width of the specimen to approximately 0.077 inch in that plane. The third slot was 0.100 inch wide and was centered in a plane containing the other slots. This geometry gave two shear planes parallel with the length of the specimen which were 1/4-inch long with a width equal to the specimen thickness.

Specimens T50-HP1B and T50-HP2B listed in Table 7 were tested in this configuration and tensile failures in the plane containing the two slots resulted. Therefore, the center slot in Specimens T50-HP3B, T50-HP5A, and T50-HP7A listed in Table 7 was placed 1/16 inch from the outer slots so that the length of the shear plane was reduced to 1/16 of an inch. Shear failures resulted when

these specimens were stressed. The nominal filament contents of these specimens are given in Table 2. Because of the density variations, the results are difficult to interpret. However, vacuum annealing does not appear to improve the interfacial shear strength appreciably. Further shear evaluations on dense specimens were planned to evaluate this relationship fully but could not be completed during the investigation. However, the shear strength of dense specimens should be higher than the 8,000 to 9,000 psi obtained for 90 percent dense specimens.

Radially Pressed Bars

Because of the difficulties encountered in obtaining dense plate specimens, a series of radially pressed cylindrical bars was prepared for an evaluation of room-temperature and elevated-temperature mechanical properties. Table 8 gives the results of mechanical data obtained on flat tensile bars with reduced-gage sections cut from the radially pressed bars. The physical properties and fabrication parameters of specimens listed in Table 8 are given in Table 5. All of the specimens listed in Table 8 had bulk densities over 97 percent of theoretical and all but specimen T50-31 were vacuum annealed at 1470 F before pressing. T50-31 was vacuum annealed at 400 F. Specimens T50-30, 31, 32, 33, and 41 were tested in the as-pressed condition at room temperature. Specimens T50-36, 37, and 38 were tested at elevated temperatures in the as-pressed condition. The last digit in the code number indicates which of three bars cut from the specimen was tested; bars numbered 1 and 3 were cut from the sides while those numbered 2 were cut from the centers of the cylindrical bars.

A comparison of the ultimate tensile strength (UTS) of Specimens T50-32, 33, and 41 with corresponding filament contents of 42, 49, and 57 volume percent reveals that the UTS increases with filament content to 49 percent but then drops as the filament content is increased to 57 percent. The UTS should increase with the volume fraction of filaments, assuming no filament damage due to the higher volume loadings occurs during fabrication. However, there appears to be a drop in strength for the specimen with a high filament content. To determine whether filament break-up was responsible for this effect, the matrix was leached from a 3/4-inch-long gage section from each of these tensile bars, and the filaments were deposited on filter paper in a Buchner funnel. A qualitative comparison of the percentage of short filaments was made by removing the bundle of long filaments and weighing the short filaments which remained on the filter paper. In addition, a microscopic examination of the short filaments was made. Approximately 10 percent of the filaments removed from each of the composites remained on the filter paper and no difference in short filament length could be detected. These results indicated that if filament break-up were a significant factor affecting the strength of the composites it could not be detected by the techniques employed.

More filament breakage and filament-filament contact probably occurs for the higher filament content. The combination of shorter filaments and filament

flaws at the contact points due to filament-filament bridging (see discussion in microstructural-stability section) probably caused the reduction in strength. Filament bridging may also have prevented the separation of the short filaments thereby preventing adequate aspect-ratio determination by the technique employed.

Specimens T50-30 exhibited very low strengths and secondary elastic moduli compared to other as-fabricated specimens prepared and tested under similar conditions. An evaluation of filament break-up by the above techniques indicated the percentage of short filaments in this sample was again about 10 percent, and no significant difference in length of the short fraction could be detected. However, microscopic examination revealed that the residue on the filter paper contained a black powdery deposit which was not present in the other specimens. This deposit and a Ni_2O_3 powder tested for comparison were insoluble in warm nitric acid. Since the volume fraction of nickel leached from this specimen was lower than that estimated on the basis of the plated weight of the filaments, the residue was believed to be Ni_2O_3. A vacuum fusion analysis was made for residual gases in this specimen and in T50-31 which was vacuum annealed at 400 F instead of 1470 F. The results indicated that the gas content of T50-30 (205 ppm oxygen, 41 ppm hydrogen, and 70 ppm nitrogen) was similar to that obtained from coated yarn during the annealing study. Specimen T50-31 had a higher gas content of 410 ppm oxygen, 74 ppm hydrogen, and 25 ppm nitrogen, yet it had a higher room-temperature strength (93,200 psi) and modulus, which suggested that residual gas in Specimen T50-30 was not responsible for its low strength (63,000 psi) and elastic modulus.

Although the reason for the anomolous low strength of T50-30 has not been determined, examination of the fracture surface under a scanning electron microscope showed that the filament content had been reduced to approximately one-half by solution and reprecipitation of carbon. Thus, the black deposit is probably recrystallized carbon, and the low strength and secondary modulus are probably due to a reduced filament content. Close examination of the filaments leached from Specimen T50-41 also revealed that a small amount of the black powdery deposit was retrieved from that sample which also had a somewhat lower strength than comparable specimens. Moreover, no deposit could be seen in the filament residue of Specimens T50-33 which had the highest room-temperature strength of the series of as-fabricated specimens. Thus, strength seemed to be related to the black deposit which was tentatively believed to be precipitated carbon. A high percentage of filament-to-filament contact points resulting from a batch of frayed yarn or in a sample with a high percentage of filaments (T50-41) could result in sintering of adjacent filaments. Thus, filament cross-overs in a specimen could contribute to solution precipitation and/or recrystallization in an apparently "normal" sample. A more detailed examination of these specimens would be necessary to evaluate fully the possible reasons for the discrepancy in their strengths and moduli.

The strengths of Specimens T50-33-1 and T50-33-3 are only about 60 percent of the composite strength calculated from the rule of mixtures. Previously 75 percent of the calculated strength was obtained.[4] These low strengths could be

caused by degradation of the strength of the filaments and/or other factors such as filament fracture during fabrication. Earlier results[4] as well as the results of other investigators indicated that both the strength and modulus of carbon filaments are degraded when the filaments are heated in contact with nickel. More recent results show that with more careful experimental techniques carbon filaments show no strength degradation when heated in contact with nickel for 1 hour up to 1800 F.[7] One of the primary factors which caused the strength reductions noted earlier seems to be a partial pressure of oxygen in the annealing furnace which is above that used for Equation (5). Based on these results, the annealing and fabrication conditions should not have degraded the strength of the filaments appreciably, but filament-filament contacts developed during fabrication could create flaws in the filaments which would lower their strength.

However, the major reason for the measured strengths and moduli being below the values predicted by the rule of mixtures is believed to be filament breakage and misalignment. Early results showed that in composites with excessive filament breakage only 50 percent of the rule of mixtures strengthening was attained.[1] Subsequent results showed that 75 percent of the rule-of-mixtures strength could be attained when filament breakage was nearly eliminated.[2] The 60 percent level attained in the present investigation appears to be a result of slightly more filament breakage than in previous specimens that gave 75 percent. Strengths representing 90 to 100 percent of rule-of-mixtures strengthening have been obtained for boron-aluminum composites, but only when fabrication conditions are controlled to (1) eliminate misaligned filaments, (2) eliminate filament breakage, (3) eliminate chemical or physical damage which would lower filament strength, and (4) when a reasonably good filament-matrix bond is achieved. Without adequate control of fabrication parameters, strengths representing 50 percent of the rule-of-mixtures strength often results.

On the basis of these results and experience in fabricating carbon-filament-reinforced nickel, the major reasons for the failure to achieve higher percentages of theoretical strengthening are (1) the low filament-metal bond strength and (2) filament breakage due to misalignment of the individual coated filaments (and plies) in the layup used for fabrication of dense composites. A more automated fabrication procedure such as continuous plating followed by alignment of plies in the preform by filament winding would probably improve composite strength. However, individual filament alignment such as is used in fabricating boron-aluminum composites is not possible with presently available carbon filaments because of their small diameters.

The elastic moduli are also below the theoretical modulus calculated from the rule of mixtures. This is also believed to be due to misaligned filaments and to a combination of low bond strength and filament breakage. Comparison of the experimental and theoretical moduli for Specimens T50-32, T50-31, and T50-41 seems to lend some support to the latter. These three specimens contain 42, 50, and 57 volume percent filaments, respectively, and show 86, 78, and 75 percent of the theoretical moduli, respectively. Since the extent of filament

breakage tends to increase with filament content, the decrease in the percentage of theoretical modulus attained as filament content is increased seems to support the hypothesis that filament breakage is contributing to modulus reduction.

The results of the elevated temperature tests conducted on Specimens T50-36, 37, and 38 are listed in Table 8. Ultimate tensile strengths decreased to about half the room-temperature value with an increase in temperature to 1800 F. At 2000 F, Specimen T50-38-2 fractured at an ultimate stress of 36,000 psi. However, the strength dropped to only 12,000 psi for Specimen T50-36-2 tested at 2200 F. Although the ultimate tensile strengths appear low, the specific strengths of the carbon-filament composites are attractive compared to other structural metals for high-temperature applications. The specific strengths (ultimate tensile strength-to-density ratio) of the specimens tested at elevated temperatures during this investigation are shown as circular points joined by the dotted curve in Figure 25. This figure also shows the specific strengths of various metals and the theoretical specific strengths of unidirectionally reinforced nickel-Thornel 50 composites with 40, 50, and 60 percent filaments for comparative purposes. Triangular points in the figure are results obtained from earlier work in which cylindrical-shaped tensile bars were tested. (4)

As discussed previously, the room-temperature strength is well below theoretical. As the test temperature is increased to 1000 and 1400 F, the strength drops to around one-half of the room-temperature value. This drop is considerably greater than that predicted by the simple rule of mixtures on the basis of a reduction of the yield strength of nickel. The exaggerated strength reduction probably occurs because of an increase in the critical pullout length combined with the fact that the filaments in the composite are not truly continuous due to breakage during fabrication. The statistical nature of the strength of the brittle carbon filaments would also tend to cause a strength reduction greater than that predicted by the rule of mixtures if the filament pullout length increased. Since the pullout length is governed by the shear strength of the nickel-carbon interface rather than the nickel yield stress, the reason for the increase in filament pullout length with temperature is not straightforward and will require further evaluation.

The data indicate that no decrease in strength occurs between 1400 and 1800. If this trend is real, it may indicate that the factor controlling filament pullout length is switching from predominantly interface shear to predominantly matrix shear.

As temperature is increased from 1800 to 2000 and 2200 F, the entire gage length of the specimen becomes part of the fracture surface. In this temperature region, the low matrix and interfacial shear strength allows the weakest points in the specimen and in each filament to be connected rather than limiting the fracture surface to a narrow zone as at lower temperatures. Thus, filament breakage, damage, and strength dispersion become more important at elevated temperatures as do inhomogeneities in the composite (areas of multiple filament fracture, areas

containing cross filament, areas of high nickel concentration, etc.). Therefore, reduction of filament breakage and further refinement of composite fabrication to reduce composite defects should increase high-temperature strength more than room-temperature strength. Such improvements could probably be attained through the development of a continuous process.

Another factor that could also result in improved composite strength at elevated temperatures is improvement in filament properties. Average strength values up to 500,000 psi have been reported on laboratory quantities of very high modulus filaments (see theoretical curve for target carbon filaments in Figure 25). Perhaps a more important consideration for high-temperature strength is the form in which the filaments are available, the continuity of the individual filaments, and the strength dispersion of the filaments. The form in which filaments can be obtained determines, to a large extent, the ability to fabricate optimum composites. Processing would be greatly simplified if larger diameter monofilaments were available, although several other inherent advantages of small-diameter filaments would be lost. Two-ply (twisted) yarns are an inconvenient form for fabrication of metal-matrix composites, since the plies must be separated and the twists removed. A tow is a more convenient form, but tows containing a smaller number of filaments than those currently available would simplify filament coating. Various continuous-processing techniques should be evaluated in conjunction with filament forms that can be produced to determine the best combination of filament and processing.

Poor load transfer to the center filaments of the specimens during testing may also have lowered the measured strength. This problem is exaggerated by the low matrix shear strength at elevated temperatures. In previous work with a different test-specimen geometry, tensile failure was not observed above 1800 F because the center core of the specimen pulled out of the conical grip section.[4] The specimen design used in the present investigation prevented this type failure, but the inability of the specimen to transfer load to the center filaments of the specimen may have reduced the measured strength considerably. If water-cooled grips were used at elevated temperatures, the matrix shear strength would be increased, thus minimizing strain lag and stress gradients. Thus, water-cooled grips could be used to determine whether stress concentrations at the outer surfaces of the specimens lower the measured strength.

Although Figure 25 indicates that the experimental tensile strength does not show a clear advantage over available materials, the potential improvements discussed above may change this situation. Also, the stress-rupture strength of the composites have the largest potential for showing improvements over available materials. However, experimental stress-rupture data on these composites have not yet been obtained.

For many high-temperature applications, stiffness rather than strength is the limiting design criterion. Figure 26 compares the specific stiffness of IN 100 to that predicted for carbon-filament-reinforced nickel. The curve shown for IN 100 is based on the measured dynamic modulus up to 1300 F and is

extrapolated to 2000 F. The experimental curve shown for nickel – 50 volume percent Thornel 50 is based on the secondary composite modulus measured at room temperature (18×10^6 psi). This extrapolation is valid for composites containing continuous filaments. The specific modulus would be expected to decrease with temperature when the composite contains broken filaments or when the stress is increased to a point where statistical filament fracture becomes significant. The extent of the reduction would be a function of the number of filament breaks per unit volume. Since the curves shown in Figure 26 for the composites are based on the secondary modulus (filament modulus times volume percentage of filaments), the contribution of the nickel matrix is neglected. At composite strains below the yield strain of the nickel matrix, the curves shown underestimate the composite modulus by about 50 percent. However, the yield strain of the nickel matrix in the temperature range shown is quite low and does not increase the stress at high strains significantly. If a compatible and less ductile alloy matrix could be developed, the matrix contribution could be quite significant at elevated temperatures.

The three remaining curves in Figure 26 show the effect of improved filament modulus on the specific properties of the composite. Thornel 50 was used in the present investigation. Thornel 75 ($E = 75 \times 10^6$ psi) is now available, as are several other carbon filaments with similar moduli. The "target" carbon filaments ($E = 100 \times 10^6$ psi) have been produced on a laboratory scale. Based on these predictions, carbon-filament-reinforced nickel should be useful for high-temperatures, stiffness-critical applications on numerous aerospace vehicles. Further advantage would be shown in applications where materials must withstand stress for appreciable times since the composite would not be expected to show appreciable plastic deformation while conventional metal would show appreciable plastic deformation at stresses well below their short-time yield stresses.

Annealed Specimens

In order to determine if postfabrication annealing affected the mechanical properties of the composite, a series of specimens was annealed 100 hours in argon at 1400, 1800, and 2200 F before testing at room temperature. During the anneal, the specimens were packed in high-purity graphite powder to prevent warping and prevent surface oxidation from residual oxygen in the furnace atmosphere. The specimens were kept in the cold end of the tube furnace until the annealing temperature was reached, then pulled into the hot zone. After the annealing treatment, the specimens were cooled rapidly by withdrawing them from the hot zone into the cold end of the furnace.

Mechanical properties of the annealed specimens given in Table 8 were determined using the self-aligning, self-tightening grips described above. The results indicate that the ultimate tensile strengths of the annealed specimens (T50-34 and T50-35) are equal to, and perhaps somewhat higher than, the strength

of similar as-fabricated specimens such as T50-31 and T50-33. In addition, the average ultimate tensile strength increases from 90,000 psi after the 1400 F anneal to 94,600 psi after 100 hours at 2200 F. Thus, thermal exposure does not degrade the mechanical strength of the composites and may actually increase it.

On the basis of the results of the microstructural-stability evaluations and on the results of other investigators, considerably different results would have been observed if a different annealing atmosphere had been used. In particular, atmospheres with a higher oxygen partial pressure than that dictated by Equation (5) would be expected to degrade the microstructure as well as the mechanical properties. Thus, claddings will be required to achieve microstructural stability in most atmospheres.

Thermally Cycled Specimens

Since many of the potential applications of carbon-filament reinforced metals would require that they be subjected to cyclic heating and cooling, a thorough evaluation of their resistance to thermal fatigue was considered necessary for design purposes. For an initial evaluation of the thermal-fatigue resistance of the carbon-filament-reinforced nickel composites, a series of specimens was thermally cycled to temperatures of 1000, 1400, and 1800 F and then tested at room temperature.

Specimens were suspended from a molybdenum wire and cycled from the hot zone to the cold zone of a vertically positioned furnace in a protective atmosphere of flowing argon. A thermocouple beaded against a test specimen indicated the specimen reached a peak temperature within 50 F of the control temperature and then cooled to a minimum temperature of about 500 F during each 4-minute cycle. To reduce oxidation of the specimens from residual oxygen in the furnace, pieces of carbon felt were attached to the wire immediately above and below each specimen. Two specimens were cycled at each temperature; one was cycled 10 times, the other 100 times. All specimens were tested in the self-aligning, self-tightening grips.

The mechanical properties of the cycled specimens are given in Table 8 for Specimens T50-39 and T50-40. Cyclic heating from 500 to 1000 F for both 10 and 100 cycles or to 1400 F for 10 cycles reduces the strength from about 95,000 psi for as-fabricated specimens to about 85,000 psi. Cycling 100 times to 1400 F or 10 times to 1800 F reduced the tensile strength to 72,700 psi and 78,800 psi, respectively. The specimen cycled 100 times to 1800 F had a strength of 58,500 psi. These results indicate that cyclic heating causes a strength reduction which increases with temperature and the number of cycles, the latter being more significant at the higher temperatures.

To evaluate the cause of the loss in strength, filaments were leached from portions of the broken tensile bars and examined microscopically. In addition, the tensile bars were sectioned near the fracture surface and were examined metallographically. No significant difference in filament break-up could be detected between any of the cycled specimens and as-fabricated specimens. However, a significant difference in microstructural characteristics was noted which is believed responsible for the loss in strength on cycling. Figures 27 and 28 show the microstructures of Specimens T50-39-3 and T50-39-1 cycled 100 times to 1000 F and 1800 F, respectively. The microstructure of the specimen cycled to 1000 F shows the small amount of porosity remaining in the specimen after fabrication, but the microstructure is essentially unchanged as a result of the cyclic heat-treatment. In contrast, Figure 28 shows that filament degradation has accompanied the cyclic heat-treatment to 1800 F. Three features can be noted in this figure which characterize the degraded microstructure. The first is that of filament rounding or the elimination of surface irregularities, the second is the formation of carbon necks or bridges between filaments, and the third is that voids can be seen around some of the filaments which suggests that interfacial separation has occurred.

The filament rounding and the filament-filament bridging can probably be explained by a solution-precipitation mechanism caused by variation of the solubility of carbon in nickel with temperature. However, the partial pressure of oxygen in the flowing-argon atmosphere in the furnace may have been well above that dictated by Equation (5) even though pieces of carbon felt were placed near the end of each specimen during cycling. If the oxygen partial pressure were high, the observed microstructural degradation in the 30-mil-thick specimens may have resulted more from the influence of oxygen in the furnace atmosphere than from a solution-precipitation reaction caused by a difference in carbon solubility with temperature.

This latter mechanism is also questionable as a result of the times involved. The time-temperature cycle of the specimen (measured with a small thermocouple welded to the specimen during cycling) showed that the specimen was at temperature for less than 1 minute on each cycle. It is doubtful that significant carbon solubility would occur in this short time interval. Further thermal-cycling evaluations are needed to determine whether the oxygen partial pressure is controlling the microstructural degradation during thermal cycling. Other thermal-cycling schedules should also be evaluated.

Assuming the oxygen partial pressure were high, the interfacial separation is probably the result of the reaction of residual oxygen in the sample with the filaments to form CO. Similar, but more severe, filament debonding was noted in the center of oxidized specimens and at the edges of specimens annealed in argon in which the partial oxygen pressure was the equilibrium value for the reaction of carbon and oxygen to form carbon monoxide.

Although cyclic heating reduced the ultimate tensile strength of the composites, the secondary elastic moduli did not show a corresponding decrease.

Thus, the elastic properties of the filaments are not degraded from thermal cycling and the loss in strength is attributed to the formation of flaws in the filaments from the solution and precipitation of carbon. Microscopic examination of the fracture surfaces of the cycled specimens revealed that little filament pullout occurred and that fracture occurred by tensile failure in a plane normal to the filament axis. This "clean" fracture was also observed only in as-fabricated Specimen T50-30 for which a low strength and elastic modulus were also obtained. This type of fracture also suggests that the filaments were weak unless the filament-metal bond was improved considerably.

CONCLUSIONS AND RECOMMENDATIONS

On the basis of the experimental work performed in this investigation, the following conclusions can be drawn.

(1) Unidirectional compaction results in more filament breakage and lower specimen densities than radial compaction of aligned bundles of nickel-coated filaments.

(2) Oxygen, nitrogen, and hydrogen impurities in nickel-coated carbon filaments prepared by electroless deposition can be reduced significantly by vacuum annealing.

(3) No significant microstructural degradation or loss of strength occurs as a result of 100-hour anneals in argon at temperatures up to 2200 F when the specimens are packed in carbon and when the coated yarn employed for specimen fabrication is vacuum annealed at 1470 F. Microstructural degradation occurs in specimens which are fabricated from nickel-coated yarn which has been vacuum annealed at 400 F. Microstructural degradation also occurs when the partial pressure of oxygen surrounding the specimen during annealing is high enough to remove carbon from solution in the nickel matrix by formation of CO.

(4) Specimens fabricated from nickel-coated yarn which has been vacuum annealed at 1470 F show a marked increase in oxidation resistance over specimens with higher gas-forming impurity contents. This phenomenon results from a decrease in the porosity formed on heating and the corresponding decrease in internal oxidation.

(5) Microstructural degradation (filament rounding) due to loss of carbon is not noticable after oxidation at 1000 F for

10 hours but penetrates to a depth of approximately 4 mils after oxidation at 1400 F for 10 hours or 1800 F for 1 hour.

(6) Claddings or the development of an alloy matrix will be required before these composites can be used for extended times at temperatures of 1400 F or above in oxidizing environments. With suitable protection from oxygen, the material is microstructually stable up to at least 2200 F.

(7) Thermal cycling in an inert atmosphere causes a loss in strength. The mechanism is not clearly understood but may be associated with the oxygen partial pressure surrounding the specimen during cycling. More work is needed to clarify this point.

(8) The room-temperature strength for a 50 volume percent filament loading is about 60 to 65 percent of that predicted from the simple rule-of-mixtures formula, and the primary and secondary moduli are approximately 75 percent of that predicted by the rule-of-mixtures formula. Both percentages decrease at higher filament loadings. The discrepancy between theoretical prediction and experimental results can probably be attributed to filament breakage and misalignment coupled with poor filament-metal bonding.

(9) Elevated-temperature strengths show a considerably greater decrease with temperature than predicted by the simple rule-of-mixtures formula. Part of this discrepancy can probably be attributed to filament breakage and part to a change in fracture mode as the shear strength of the matrix decreases.

(10) Data are needed on the stress-rupture and fatigue resistance to evaluate more fully the potential of the material.

(11) Improvements can be expected from development of continuous, automated processing and from the availability of improved filaments with improved properties and more optimum forms. With these improvements, the material will offer significant advantages over available materials in specific stiffness and probably specific strength at temperatures between 1000 F and 2200 F.

Future work on these materials should include:

(1) Development of continuous automated processing

(2) Investigation of the mechanism responsible for strength degradation due to thermal cycling

(3) Development of claddings or an alloy matrix that will prevent loss of carbon through surface reaction with oxygen

(4) Development of improved filament-metal bond strength

(5) Evaluation of stress-rupture strength, fatigue strength, and impact resistance as well as additional high-temperature-strength data

(6) Evaluation of the off-axis properties and the properties of cross-plied materials.

TIME EXPENDITURES

The total time expenditure (man hours) for this research program was as follows:

Supervision	114
Research Engineers and Scientists	1253
Laboratory Technicians	2228
Other	846
TOTAL	4441

These figures are based on the total time charged to the project plus an estimate of the time involved in processing the final report.

REFERENCES

(1) Niesz, D. E., Fleck, J. N., and Kistler, C. W., Jr., "Development of Filament-Reinforced Metals", Final Report, Contract NOw-65-0615-c, AD-649509, January, 1967.

(2) Kostas, G. J., "Liquid Phase Deposition of Metals From Organometallic Compounds – Its Future and Limitations", Paper presented at International Symposium on Decomposition of Organometallic Compounds to Refractory Ceramics, Metals, and Metal Alloys, Dayton, Ohio, November 28-30, 1967.

(3) "Typical Properties and Reactions of Aluminum Diethyl Hydride", Technical Bulletin, Continental Oil Company, Houston, Texas.

(4) Niesz, D. E., "Development of Carbon-Filament-Reinforced Metals", Final Report, Contract N00019-67-C-0342, AD-836794, June, 1968.

(5) Dini, J. W. and Coronado, P. R., "Thick Nickel Deposits of High Purity by Electroless Methods", Plating, 54 (4), 385-90 (1967).

(6) Metals Handbook, 1948 Edition, Published by The American Society for Metals, Taylor Lyman, editor.

(7) Jackson, P. W., "Some Studies of the Compatibility of Graphite and Other Fibers With Metal Matrices", paper presented at 1969 Western Metal and Tool Conference and Exposition, Los Angeles, California, March 10-13, 1969.

(8) H. W. Rauch, Sr., W. H. Sutton, and L. R. McCreight, "The Fabrication, Testing, and Application of Fiber-Reinforced Materials: A Survey", Technical Report AFML-TR-68-162, Contract AF33(615)-3278, September, 1968.

(9) "Metallurgical and Mechanical Properties of Titanium Alloy Ti, 6Al, 2Sn, 4Zr, 2Mo Sheet and Bar Forgings", Timet Technical Bulletin, September, 1966.

(10) "High Temperature/High Strength Nickel Base Alloys", International Nickel Company Bulletin (1964).

(11) "Metallurgy and Properties of Thoria-Strengthened Nickel", Defense Metals Information Center Memorandum 210 (October, 1965).

(12) Aerospace Structural Metals Handbook, Volume II-A, Nonferrous Alloys, ASD-TDR-63-741, March, 1967.

TABLE 1. GAS CONTENT AND WEIGHT CHANGE OF NICKEL-COATED YARN AFTER VARIOUS ANNEALING CYCLES

Atmosphere	Temperature, F	Gas Analysis, ppm			Weight Change, percent
		O_2	H_2	N_2	
As-plated yarn		1550	125	450	--
Hydrogen	1700	470	15	10	-12.3
Hydrogen-methane	1110	535	22	130	0.0
Hydrogen-methane	1300	365	22	85	+0.3
Hydrogen-methane	1470	385	43	20	+10.5
Vacuum, 2×10^{-2} torr	750	2150	45	120	-0.29
Vacuum, 5×10^{-3} torr	1110	--	--	--	-0.24
Vacuum, 2×10^{-1} torr	1470	520	25	20	-0.45
Vacuum, 5×10^{-3} torr	1470	240	11	10	-0.28
Vacuum, 5×10^{-3} torr	1650	--	--	--	-0.34
Vacuum, 2×10^{-2} torr	1830	1210	18	110	-0.69
Vacuum, 5×10^{-3} torr	1830	175	14	5	-0.27

TABLE 2. RESULTS OF AUTOCLAVE RUN 1

Specimen	Nickel, volume percent	Vacuum Annealing Temperature, F	Bulk Density, percent of theoretical
T50-HP1	53	None	94
T50-HP2	54	1110	90
T50-HP3	56	1470	87
T50-HP4	54	1470	88
T50-HP5	60	1650	80
T50-HP6	59	1650	No deformation
T50-HP7	60	1830	93

TABLE 3. RESULTS OF AUTOCLAVE RUN 2

Specimen	Nickel, volume percent	Vacuum Annealing Temperature, F	Bulk Density, percent of theoretical	Remarks
T50-HP8	50	1470	83	Lid failure
T50-HP9	50	1470	--	Weld failure
T50-HP10	51	1470	--	Lid failure
T50-HP11	50	1470	78	Lid failure
T50-HP12	50	1470	--	Weld failure
T50-HP13	54	1470	--	Lid failure
T50-HP14	52	1470	--	Lid failure
T50-HP15	50	1470	--	Lid failure
T50-HP16	50	1470	83	No visible crack
T50-HP17	50	400	--	Weld failure

TABLE 4. RESULTS OF AUTOCLAVE RUN 3

Specimen	Nickel, volume percent	Vacuum Annealing Temperature, F	Bulk Density, percent of theoretical
T50-HP18	50	1470	97
T50-HP19	50	1470	91
T50-24	52	1470	99
T50-25	52	1470	100
T50-26	49	1470	100
T50-27	49	400	100

TABLE 5. SUMMARY OF FABRICATION PARAMETERS, PHYSICAL PROPERTIES, AND INTENDED USE OF CYLINDRICAL SPECIMENS

Specimen	Nickel, volume percent	Swaged Density, percent of theoretical	Vacuum Anneal[a] Temperature, F	Vacuum Anneal[a] Time, hours	Autoclave Run[b]	Bulk Density, percent of theoretical	Use
T50-24	52	85	1470	1	3	99	Not used - overswaged
T50-25	52	85	1470	1	3	100	Not used - overswaged
T50-26	49	85	1470	1	3	100	Microstructural stability
T50-27	49	85	400	1	3	100	Microstructural stability
T50-28	55	71	400	2	4	97	Oxidation resistance
T50-29	57	72	1470	2	4	103	Oxidation resistance
T50-30	50	68	1470	2	4	104	Fabrication study
T50-31	50	71	400	2	4	98	Fabrication study
T50-32	58	70	1470	2	4	100	Fabrication study
T50-33	51	71	1470	2	4	100	High-temperature strength
T50-34	52	68	1470	2	4	101	100-hour argon anneal
T50-35	52	69	1470	2	4	99	100-hour argon anneal
T50-36	50	71	1470	2	4	100	High-temperature strength
T50-37	50	68	1470	2	5	100	High-temperature strength
T50-38	52	67	1470	2	5	101	High-temperature strength
T50-39	52	68	1470	2	5	100	Thermal fatigue
T50-40	53	67	1470	2	5	101	Thermal fatigue
T50-41	43	70	1470	2	5	101	Fabrication study

(a) Vacuum of 5×10^{-3} torr or better for all specimens.

(b) Autoclave Runs 3, 4, and 5 were equivalent and consisted of 1 hour at 5000 psi and 1830 F; see text for details of pressing cycle.

TABLE 6. RESULTS OF TENSILE TESTS ON UNIAXIALLY PRESSED PLATE SPECIMENS

Specimen	Fracture Stress, psi	Secondary Modulus, 10^6 psi	Facing Pad	Remarks
T50-HP1B	(57,600)	15.0	None	Pulled from grip; failed at a lower stress in grip when grip was tightened
T50-HP2B	56,000	13.0	320-grit emery cloth	Gage failure
T50-HP3B	46,200	13.0	5-mil aluminum foil	Failed in grip
T50-HP3A	65,000	15.0	None	Gage failure
T50-HP5A	52,000	14.8	320-grit emery cloth	Gage failure
T50-HP7A	67,000	12.8	320-grit emery cloth	Failed at end of grip

TABLE 7. RESULTS OF INTERFACIAL SHEAR-STRENGTH EVALUATIONS ON UNIAXIALLY PRESSED PLATE SPECIMENS

Specimen	Bulk Density, percent of theoretical	Vacuum Annealing Temperature, F	Shear Strength, psi	Remarks
T50-HP1B	94	None	8,000	Tensile failure
T50-HP2B	90	1110	7,750	Tensile failure
T50-HP3B	87	1470	9,100	Shear failure
T50-HP5A	80	1650	6,300	Shear failure
T50-HP7A	93	1830	8,700	Shear failure

TABLE 8. RESULTS OF TENSILE TESTS ON FLAT SPECIMENS CUT FROM RADIALLY PRESSED BARS

Specimen	Test Temperature	Nickel, volume percent	Condition	Ultimate Tensile Strength[a], psi	Primary Modulus[b], 10^6 psi	Transition Strain, percent	Secondary Modulus[c], 10^6 psi	Elongation, percent	Remarks
T50-30-1	Room	50	As-Pressed	--	--	--	--	--	Failed at pin while aligning
30-2	Ditto	50	Ditto	62,500	30.5	0.070	9.6	0.505	Tensile failure (bolt tighten grips)
30-3	"	50	"	64,300	28.4	0.135	9.7	0.415	Tensile failure
T50-31-1	"	50	"	93,200	33.5	0.085	17.1	0.465	Tensile/shear (bolt tighten grips)
31-2	"	50	"	77,200	26.9	0.085	18.0	0.380	Tensile (poor alignment)
31-3	"	50	"	--	--	--	--	--	Spare (not tested)
T50-32-1	"	58	"	78,500	29.7	0.105	17.6	0.375	Tensile failure (bolt tighten grips)
32-2	"	58	"	79,600	27.6	0.115	17.3	0.390	Tensile failure
32-3	"	58	"	--	--	--	--	--	Spare (not tested)
T50-33-1	"	51	"	95,400	--	--	--	--	Tensile/shear (bolt tighten grips)
33-2	"	51	"	--	--	--	--	--	Spare (not tested)
33-3	"	51	"	98,000	--	--	--	--	Tensile failure
T50-34-1	"	52	Annealed at 100 hr at 1400 F	89,100	29.2	0.095	18.0	0.45	Tensile/shear
34-2	"	52	1800 F	95,500	34.1	0.058	18.4	0.43	Tensile/shear
34-3	"	52	2200 F	91,600	26.5	0.050	17.1	0.505	Tensile/shear
T50-35-1	"	52	1400 F	91,300	31.1	0.055	17.9	0.465	Tensile failure
35-2	"	52	1800 F	92,500	32.0	0.055	18.7	0.465	Tensile/shear
35-3	"	52	2200 F	97,700	26.0	0.070	18.1	0.51	Tensile/shear
T50-36-1	1000 F	51	As-Pressed	78,400	--	--	--	--	Tensile/shear in grip (poor alignment)
36-2	2200 F	51	Ditto	11,600	--	--	--	--	Progressive filament pull-out in gage
36-3	1800 F	51	"	52,600	--	--	--	--	Tensile/shear
T50-37-1	1000 F	50	"	80,800	--	--	--	--	Tensile/shear
37-2	1800 F	50	"	38,600	--	--	--	--	Tensile failure
37-3	1400 F	50	"	56,200	--	--	--	--	Tensile/shear (poor alignment)
T50-38-1	1400 F	52	"	41,800	--	--	--	--	Tensile/shear
38-2	2000 F	52	"	35,700	--	--	--	--	Tensile/shear in gage section
38-3	--	52	"	--	--	--	--	--	Spare (not tested)
T50-39-1	Room	52	Cycled from 500 F to 1800 F(100)	58,500	24.0	0.070	16.1	0.335	Tensile/shear
39-2	Ditto	52	1400 F(100)	72,700	25.3	0.080	17.3	0.375	Tensile failure
39-3	"	52	1000 F(100)	87,300	25.6	0.078	15.9	0.52	Tensile failure
T50-40-1	"	53	1800 F(10)	78,800	29.3	0.080	16.6	0.42	Tensile failure
40-2	"	53	1400 F(10)	84,100	29.3	0.055	17.5	0.43	Tensile failure
40-3	"	53	1000 F(10)	85,400	27.6	0.083	16.8	0.47	Tensile failure in gage section
T50-41-1	"	43	As-Pressed	81,600	28.5	0.100	20.8	0.35	Tensile/shear (200 mesh TiC grit)
41-2	"	43	Ditto	--	--	--	--	--	Shear failure in grip at 64,000 psi
41-3	"	43	"	90,500	29.8	0.105	20.5	0.385	Tensile/shear

(a) Theoretical values (calculated from filament strength of 293,000 psi and matrix yield stress of 30,000 psi at fracture) range from 140,000 to 175,000 psi for specimens with matrix volume percentages of 58 and 43 percent, respectively.

(b) Theoretical values (calculated from filament modulus of 48×10^6 psi and matrix modulus of 30×10^6 psi) range from 37.6×10^6 to 40.3×10^6 psi for above matrix percentages.

(c) Theoretical values range from 20.2×10^6 to 27.4×10^6 psi assuming no contribution from matrix.

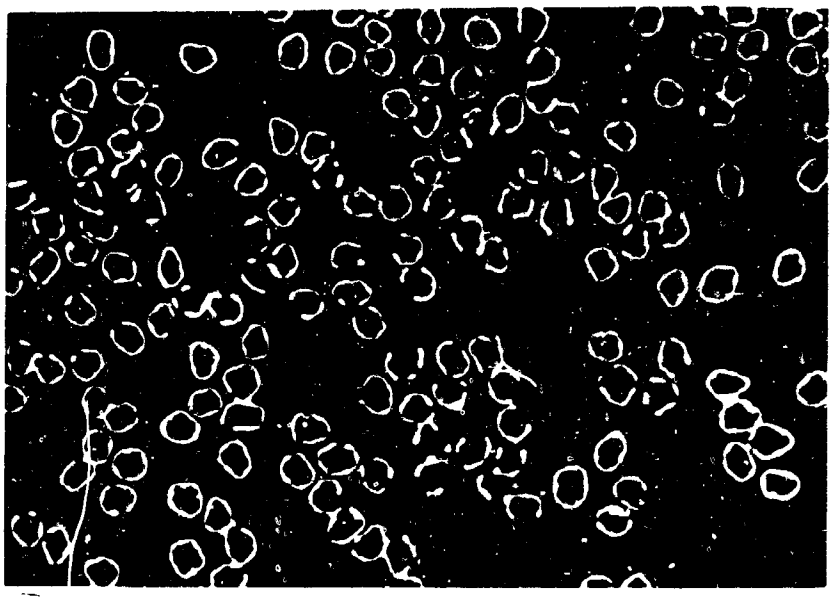

500X As Polished 2D527

FIGURE 1. NICKEL-COATED YARN AFTER ANNEALING IN VACUUM OF 2×10^{-2} TORR AT 1830 F

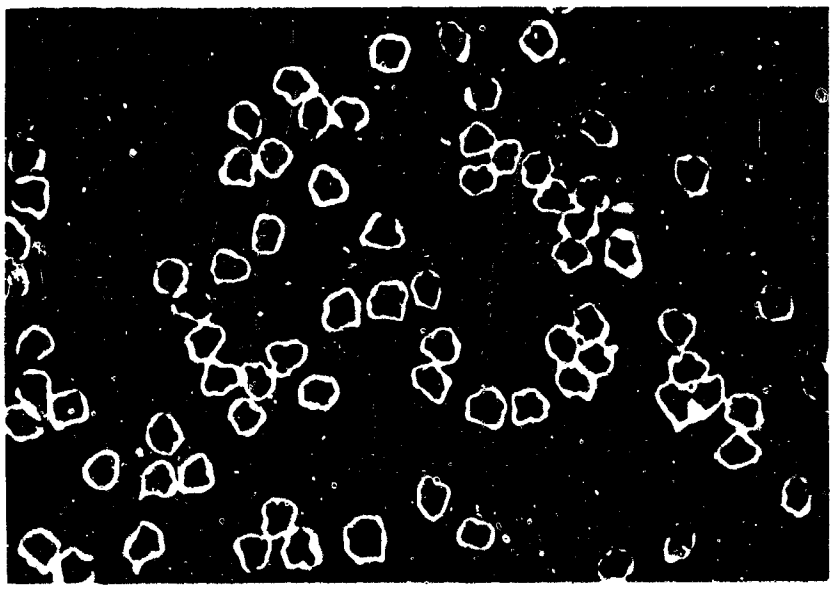

500X As Polished 2D647

FIGURE 2. NICKEL-COATED YARN AFTER ANNEALING IN VACUUM OF BETTER THAN 5×10^{-3} TORR AT 1470 F

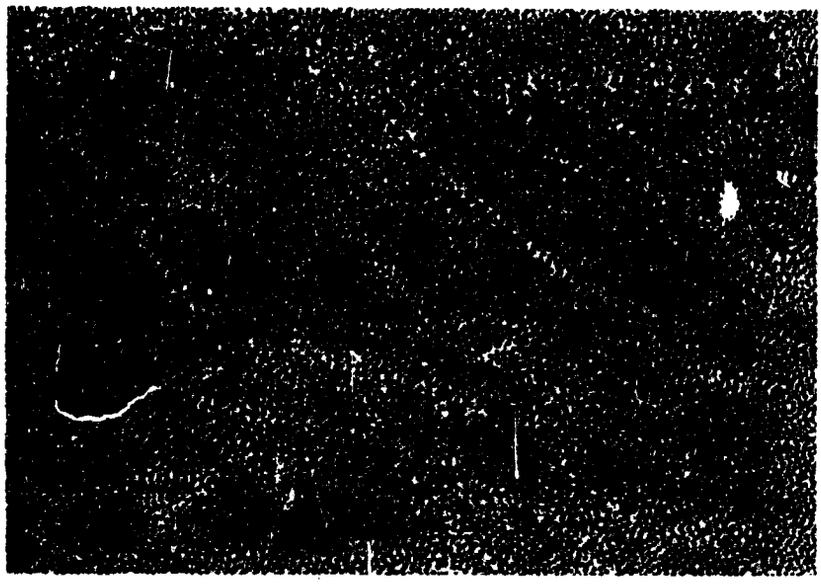

100X As Polished 9D512

FIGURE 3. MICROSTRUCTURE IN CENTER OF SPECIMEN T50-26 ANNEALED 100 HOURS IN ARGON AT 1400 F

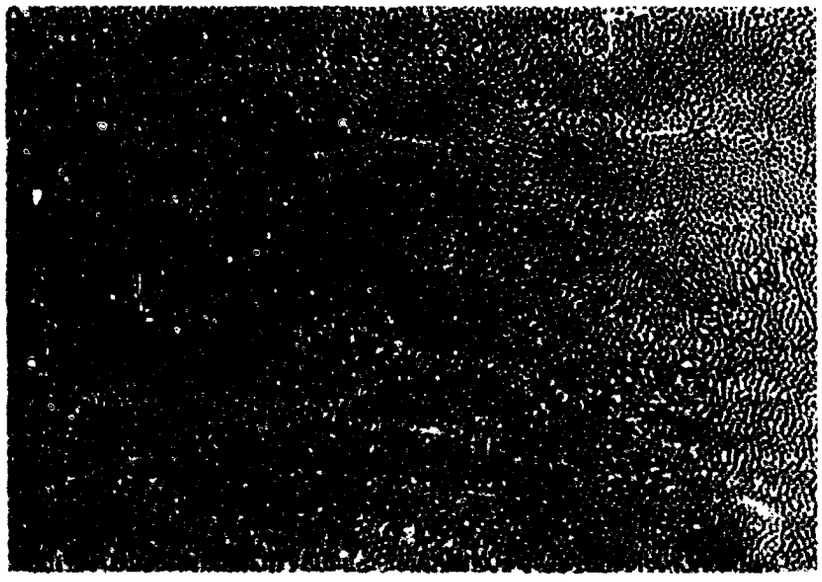

100X As Polished 9D516

FIGURE 4. MICROSTRUCTURE IN CENTER OF SPECIMEN T50-27 ANNEALED 100 HOURS IN ARGON AT 1400 F

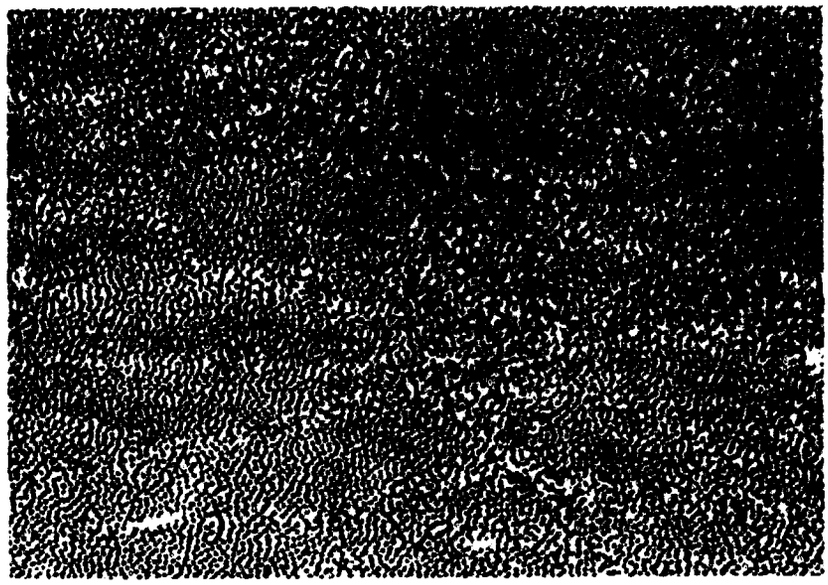

100X As Polished 9D511

FIGURE 5. MICROSTRUCTURE IN CENTER OF SPECIMEN T50-26 ANNEALED 100 HOURS IN ARGON AT 1800 F

100X As Polished 9D515

FIGURE 6. MICROSTRUCTURE IN CENTER OF SPECIMEN T50-27 ANNEALED 100 HOURS IN ARGON AT 1800 F

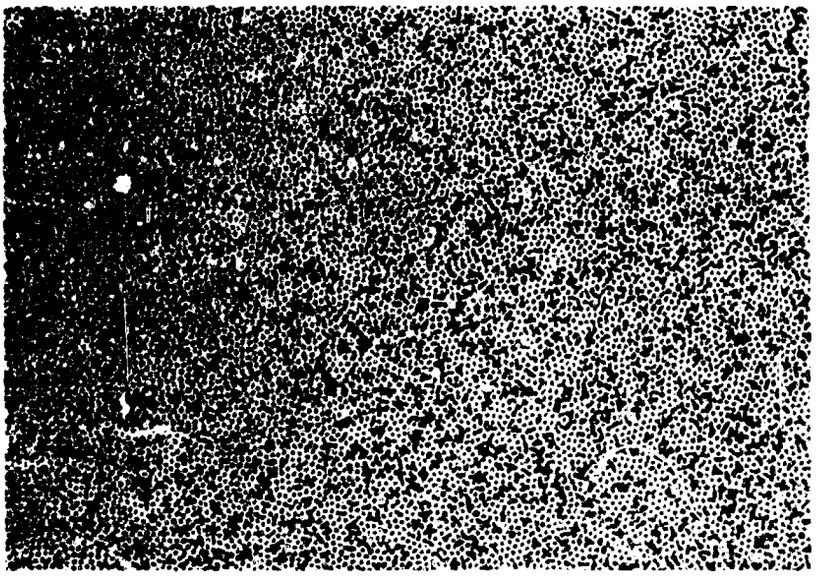

100X As Polished 9D514

FIGURE 7. MICROSTRUCTURE IN CENTER OF SPECIMEN T50-28 ANNEALED 100 HOURS IN ARGON AT 2200 F

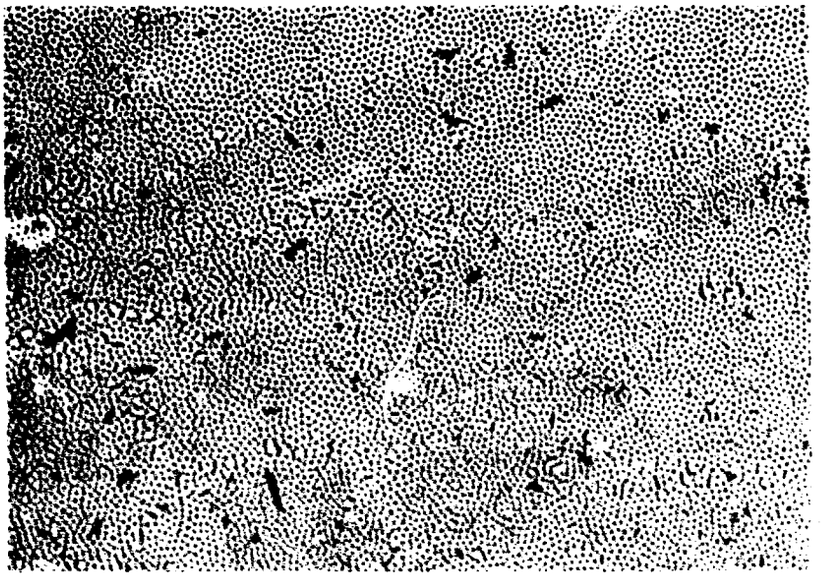

100X As Polished 9D510

FIGURE 8. MICROSTRUCTURE IN CENTER OF SPECIMEN T50-29 ANNEALED 100 HOURS IN ARGON AT 2200 F

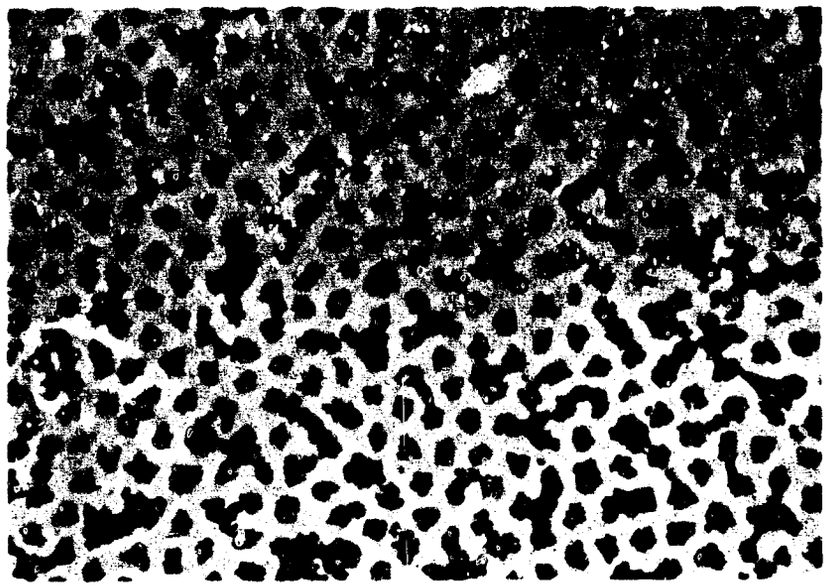

500X As Polished 9D519

FIGURE 9. TYPICAL MICROSTRUCTURE IN CENTER OF SPECIMEN T50-28 ANNEALED 100 HOURS IN ARGON AT 2200 F

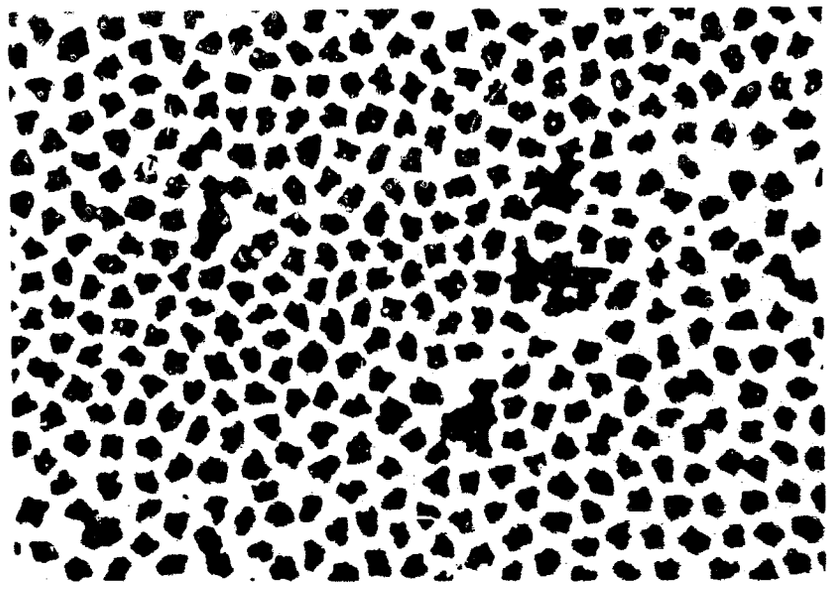

500X As Polished 9D522

FIGURE 10. TYPICAL MICROSTRUCTURE IN CENTER OF SPECIMEN T50-29 ANNEALED 100 HOURS IN ARGON AT 2200 F

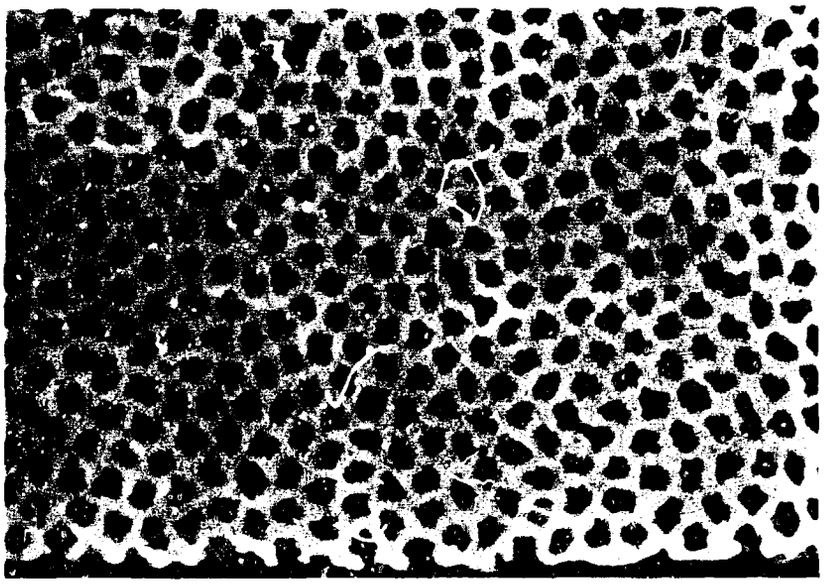

500X As Polished 9D525

FIGURE 11. MICROSTRUCTURE AT EDGE OF SPECIMEN T50-28 ANNEALED 100 HOURS IN ARGON AT 2200 F

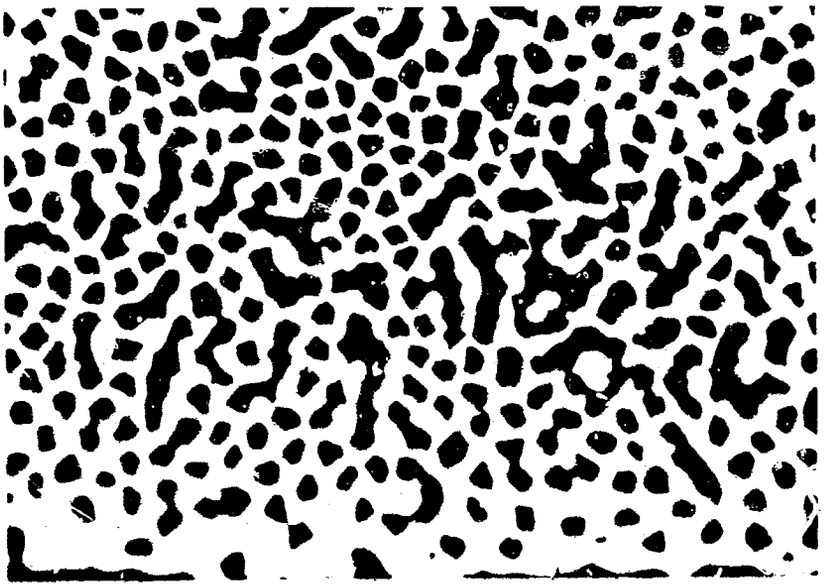

500X As Polished 9D526

FIGURE 12. MICROSTRUCTURE AT EDGE OF SPECIMEN T50-27 ANNEALED 10 HOURS IN ARGON AT 2200 F

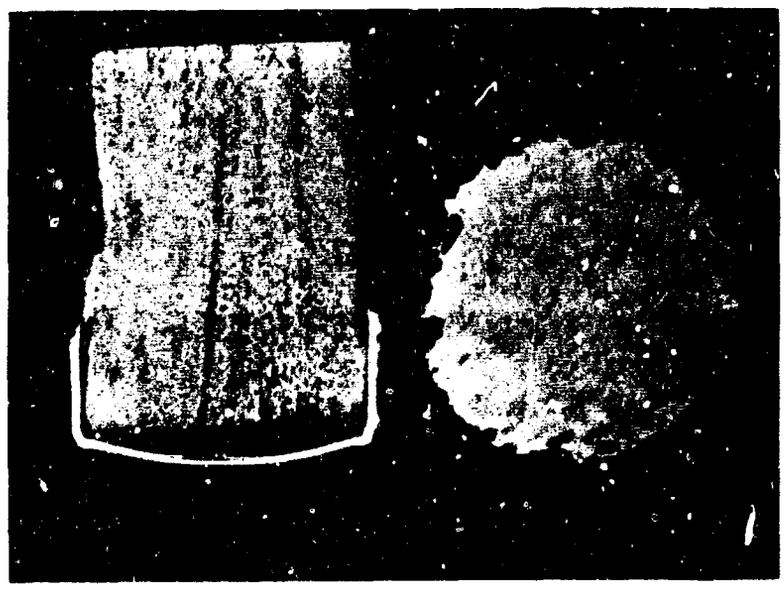

10X As Polished 2D540

FIGURE 13. MACROSTRUCTURE OF NICKEL-PLATED SPECIMEN OXIDIZED 10 HOURS IN AIR AT 1400 F

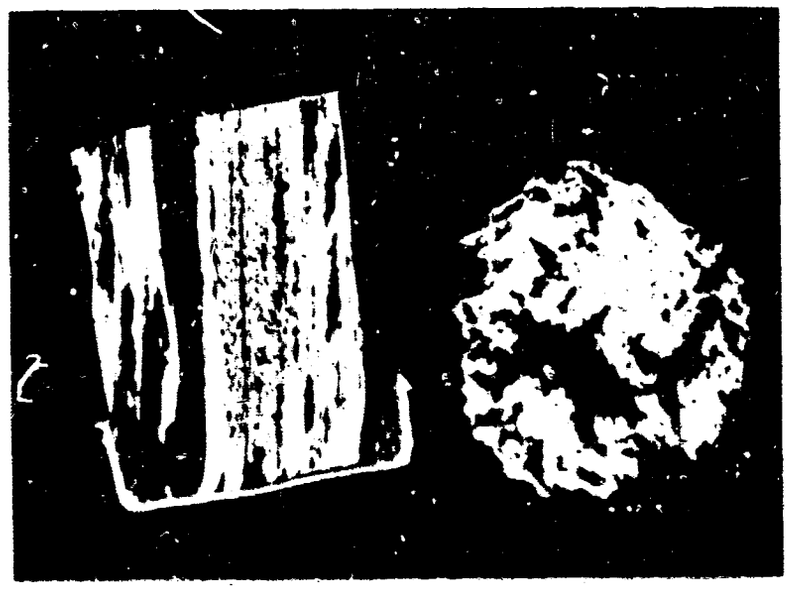

10X As Polished 2D538

FIGURE 14. MACROSTRUCTURE OF NICKEL-PLATED SPECIMEN OXIDIZED 10 HOURS IN AIR AT 1800 F

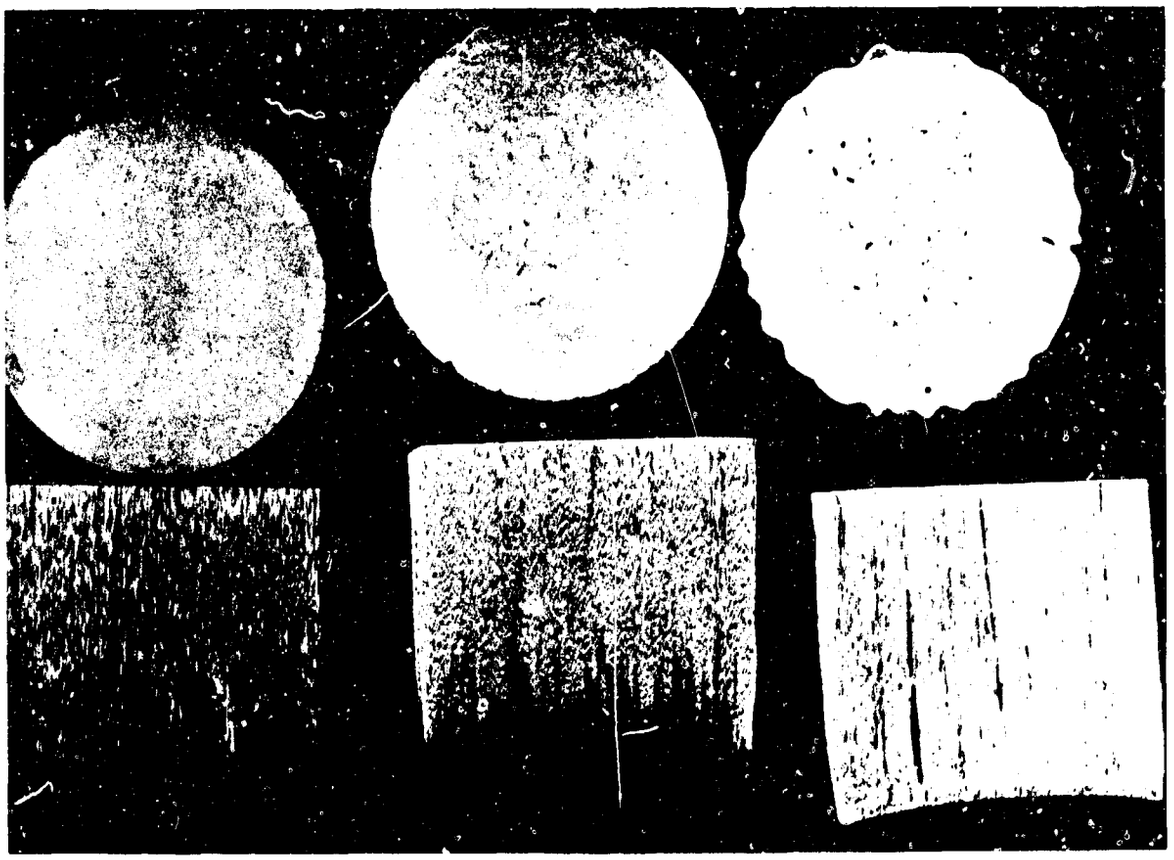

10X As Polished 9D482

a. 1000 F b. 1400 F c. 1800 F

FIGURE 15. MACROSTRUCTURE OF SPECIMEN T50-28 OXIDIZED 10 HOURS IN AIR

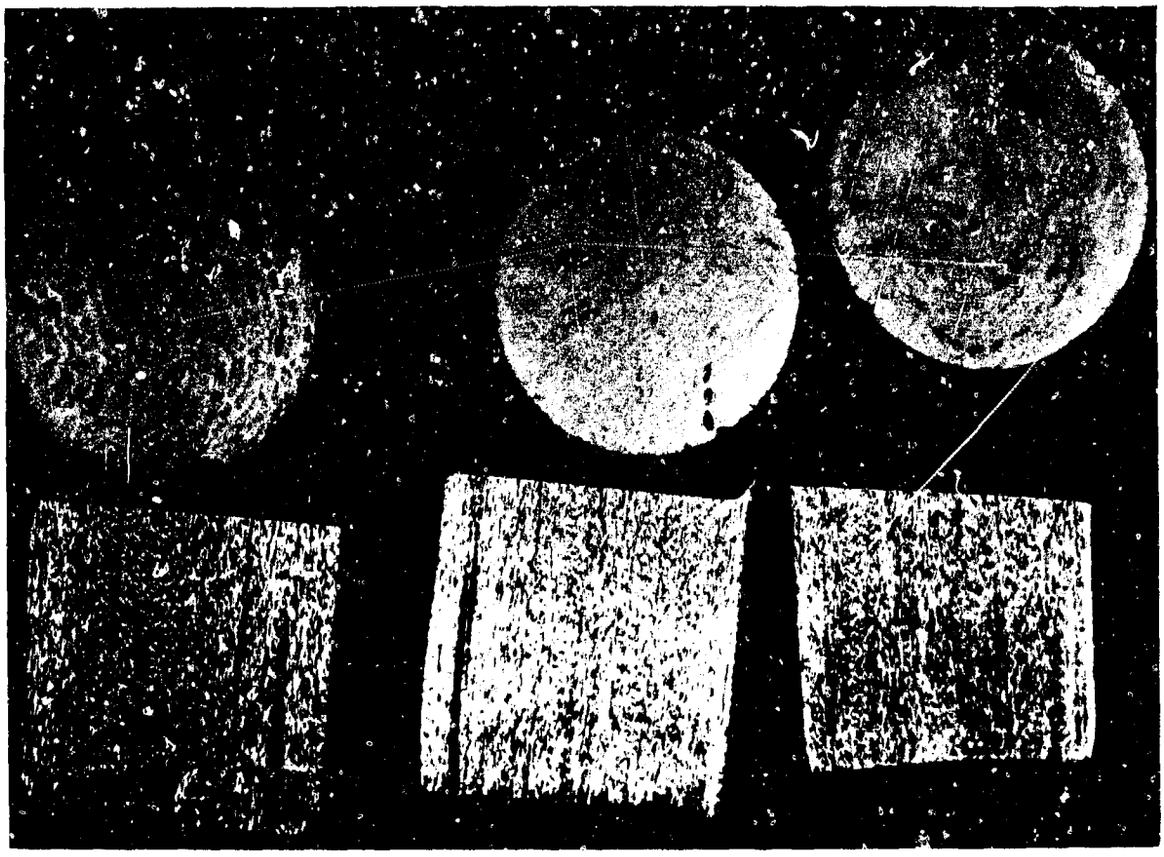

10X As Polished 9D484

a. 1000 F b. 1400 F c. 1800 F

FIGURE 16. MACROSTRUCTURE OF SPECIMEN T50-29 OXIDIZED 10 HOURS IN AIR

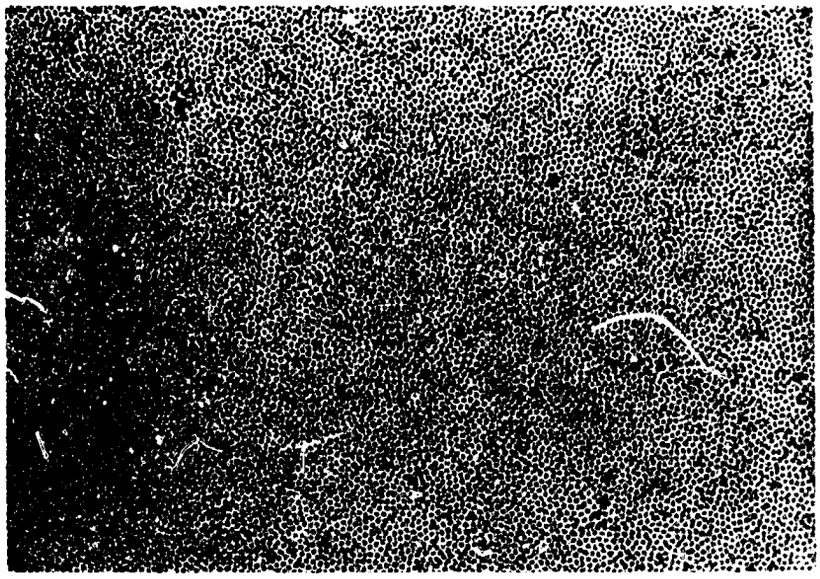

100X As Polished 9D465

FIGURE 17. MICROSTRUCTURE IN CENTER OF SPECIMEN T50-28 OXIDIZED 10 HOURS IN AIR AT 1000 F

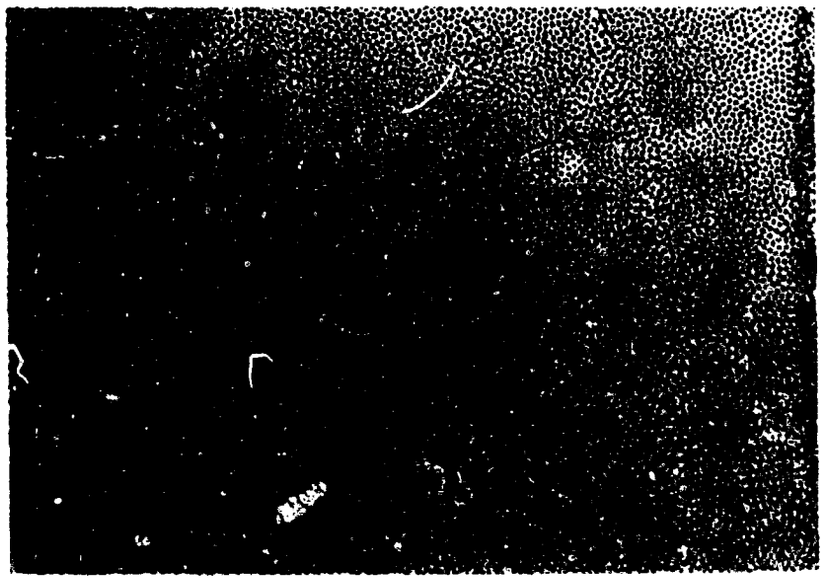

100X As Polished 9D462

FIGURE 18. MICROSTRUCTURE IN CENTER OF SPECIMEN T50-29 OXIDIZED 10 HOURS IN AIR AT 1000 F

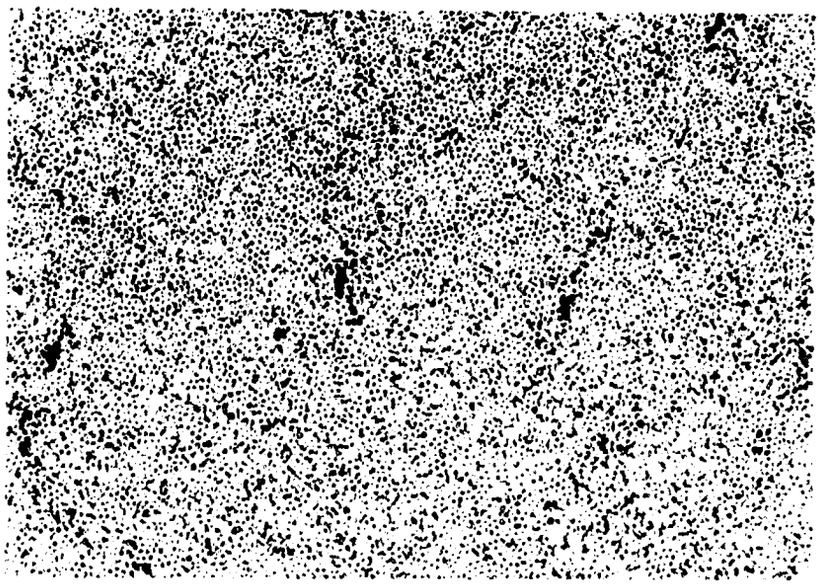

100X As Polished 9D466

FIGURE 19. MICROSTRUCTURE IN CENTER OF SPECIMEN T50-28 OXIDIZED 10 HOURS IN AIR AT 1400 F

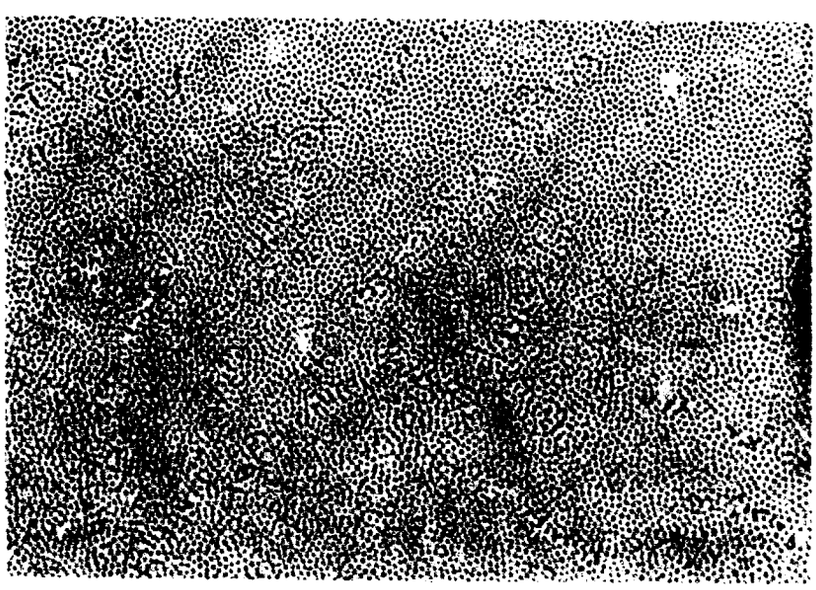

100X As Polished 9D463

FIGURE 20. MICROSTRUCTURE IN CENTER OF SPECIMEN T50-29 OXIDIZED 10 HOURS IN AIR AT 1400 F

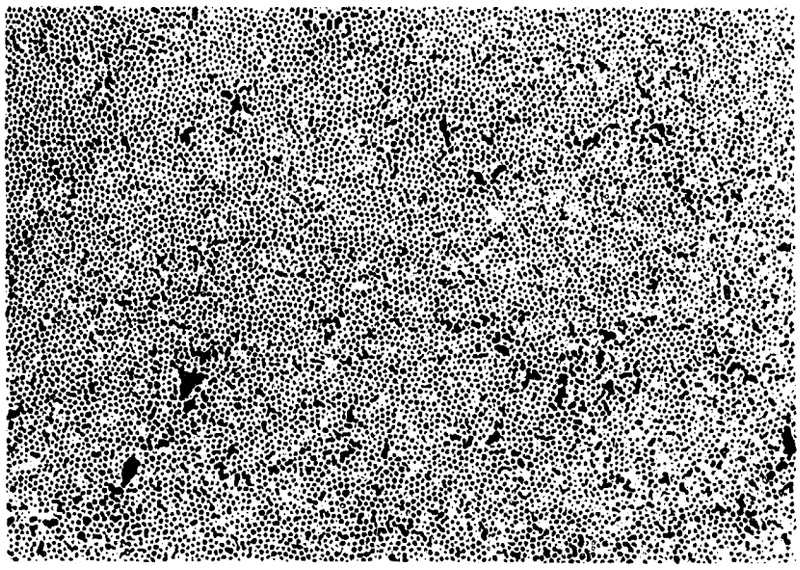

100X As Polished 9D467

FIGURE 21. MICROSTRUCTURE IN CENTER OF SPECIMEN T50-28 OXIDIZED 10 HOURS IN AIR AT 1800 F

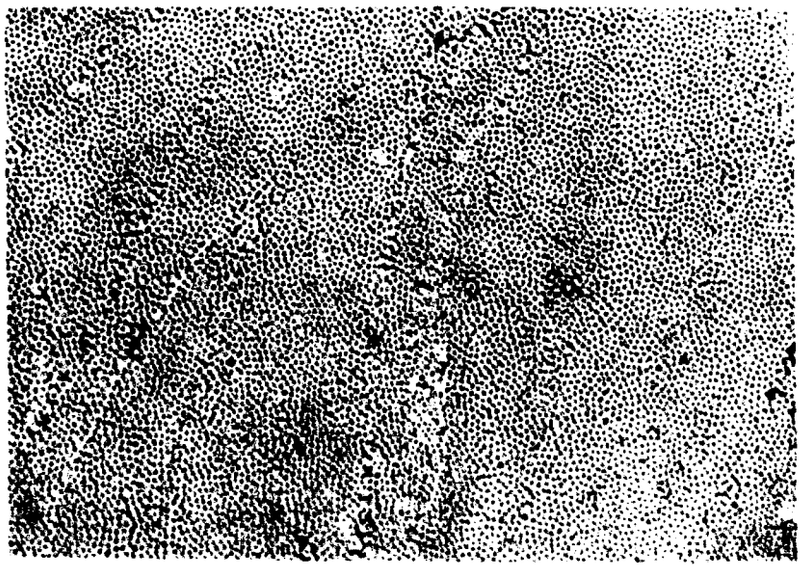

100X As Polished 9D464

FIGURE 22. MICROSTRUCTURE IN CENTER OF SPECIMEN T50-29 OXIDIZED 10 HOURS IN AIR AT 1800 F

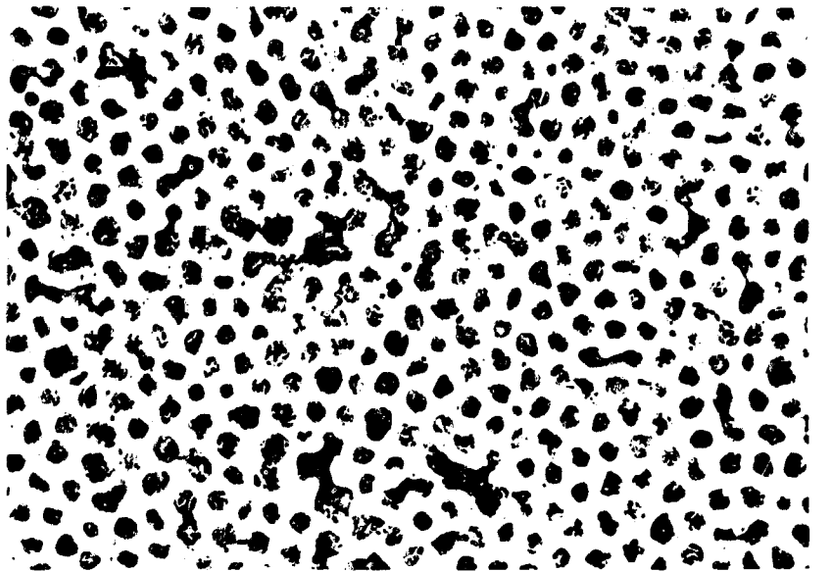

500X As Polished 9D480

FIGURE 23. MICROSTRUCTURE IN CENTER OF SPECIMEN T50-28 OXIDIZED 10 HOURS IN AIR AT 1800 F

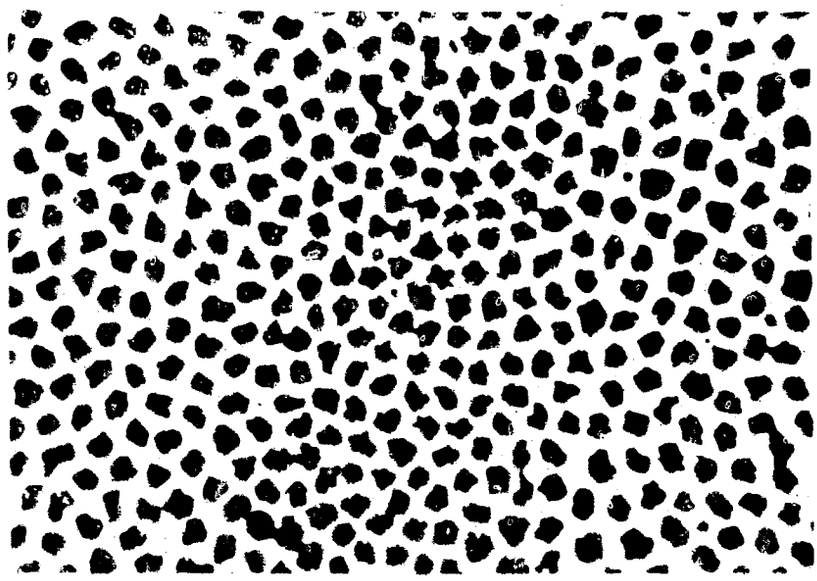

500X As Polished 9D477

FIGURE 24. MICROSTRUCTURE IN CENTER OF SPECIMEN T50-29 OXIDIZED 10 HOURS IN AIR AT 1800 F

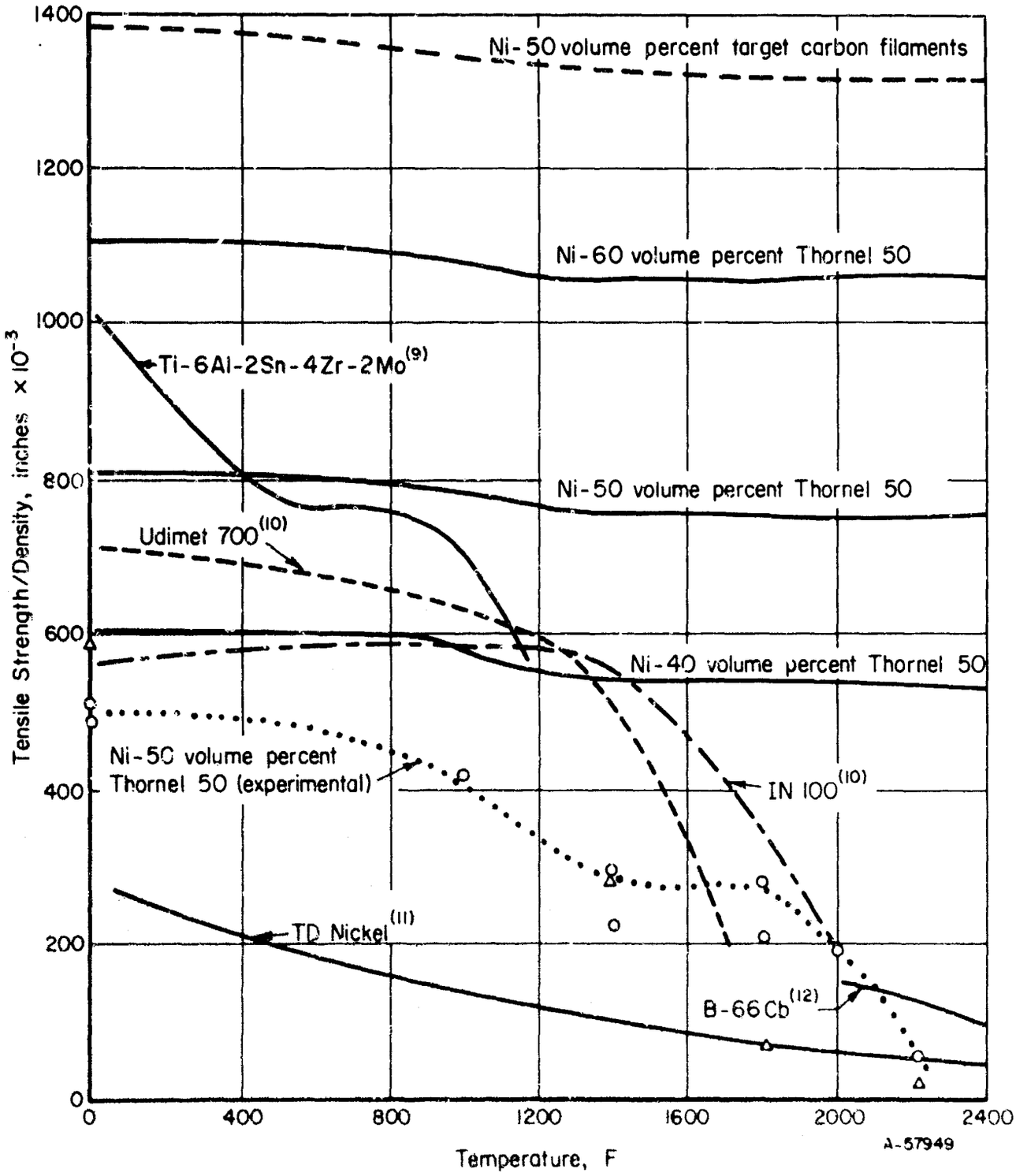

FIGURE 25. THEORETICAL AND EXPERIMENTAL STRENGTH/DENSITY AS A FUNCTION OF TEMPERATURE OF CARBON-FILAMENT-REINFORCED NICKEL COMPARED TO PUBLISHED DATA FOR VARIOUS METALS

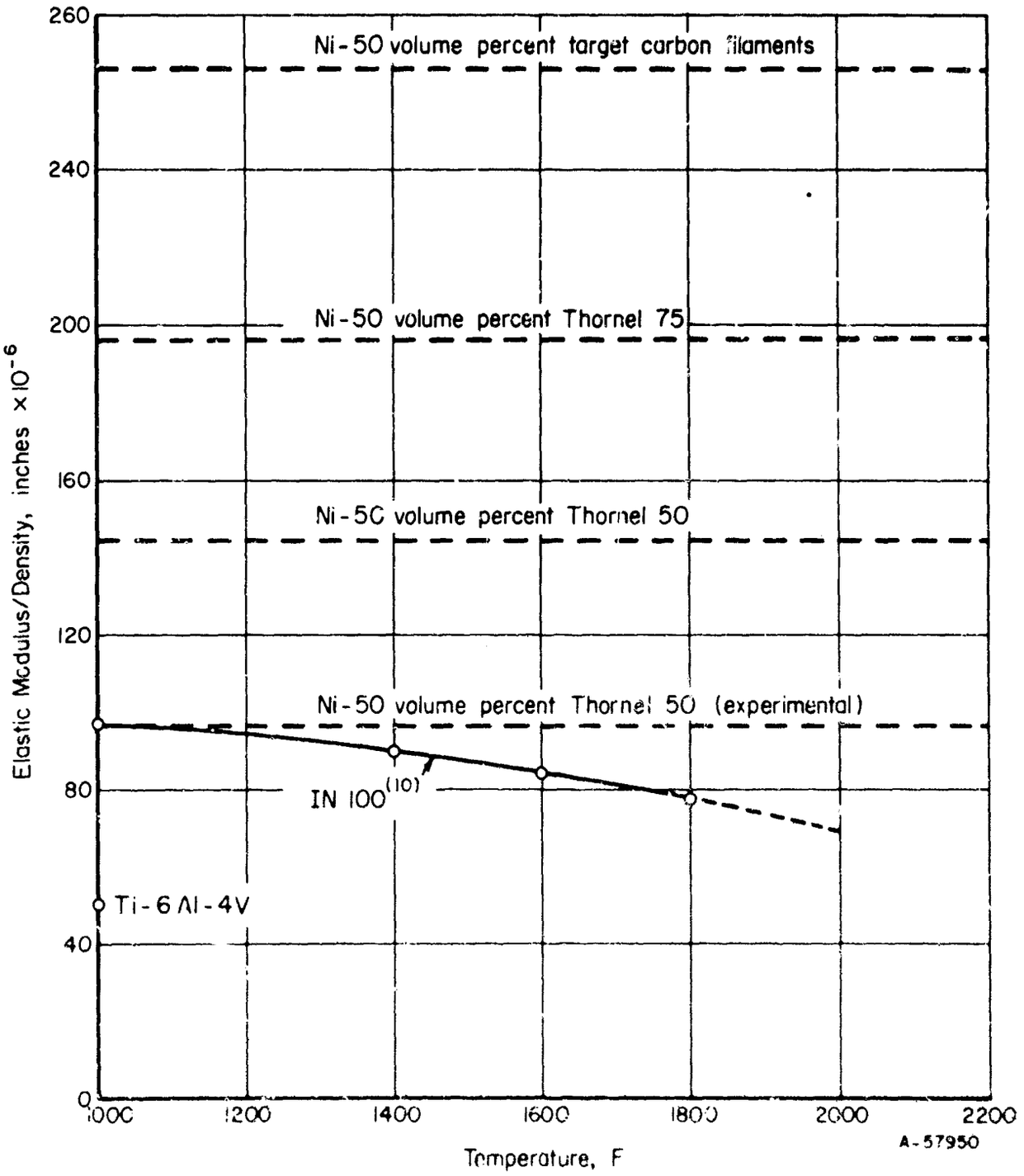

FIGURE 26. THEORETICAL ELASTIC MODULUS/DENSITY AS A FUNCTION OF TEMPERATURE FOR CARBON-FILAMENT-REINFORCED NICKEL COMPARED TO PUBLISHED DATA FOR SELECTED METALS

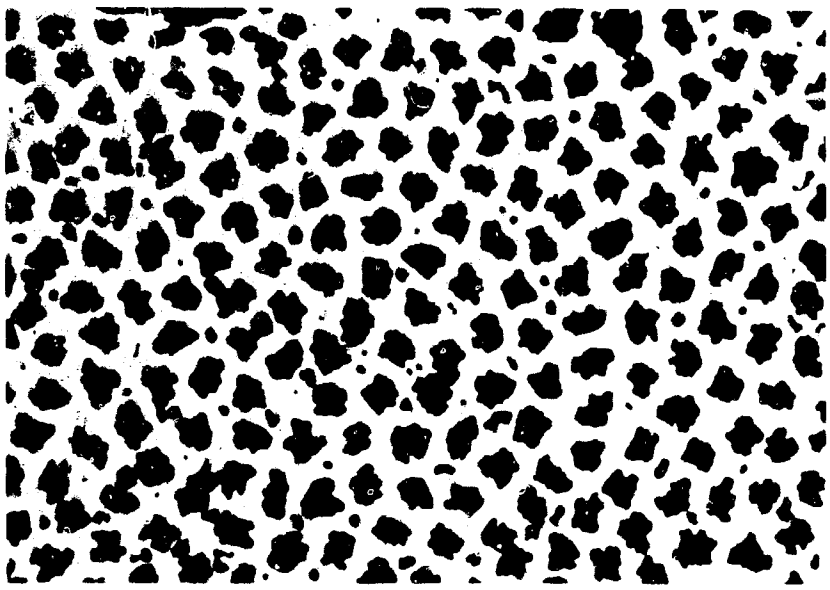

750X As Polished 9D891

FIGURE 27. MICROSTRUCTURE IN CENTER OF SPECIMEN T50-39-3 CYCLED 100 TIMES TO 1000 F

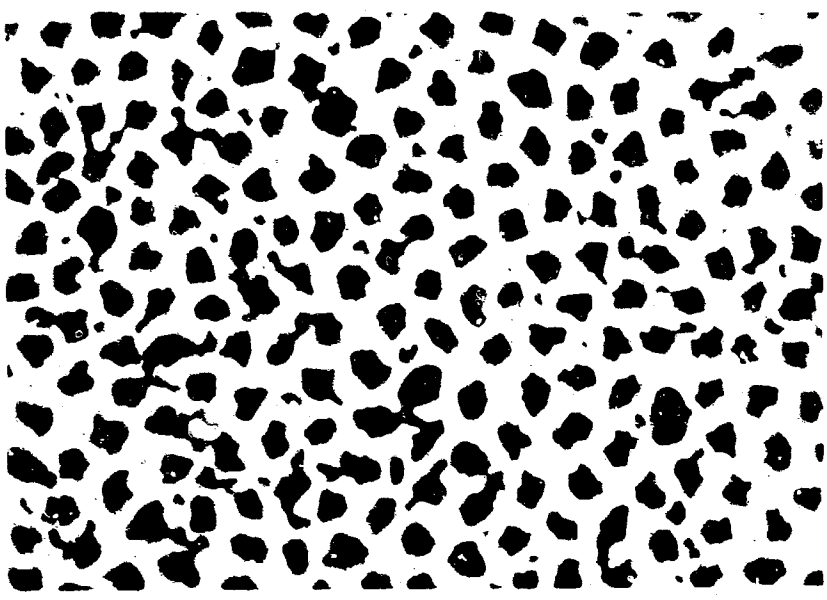

750X As Polished 9D889

FIGURE 28. MICROSTRUCTURE IN CENTER OF SPECIMEN T50-39-1 CYCLED 100 TIMES TO 1800 F

Unclassified

Security Classification

DOCUMENT CONTROL DATA - R&D

(Security classification of title, body of abstract and indexing annotation must be entered when the overall report is classified)

1. ORIGINATING ACTIVITY (Corporate author)

Battelle Memorial Institute
Columbus Laboratories
505 King Avenue, Columbus, Ohio

2a. REPORT SECURITY CLASSIFICATION

Unclassified

2b. GROUP

None

3. REPORT TITLE

Development of Carbon-Filament-Reinforced Metals

4. DESCRIPTIVE NOTES (Type of report and inclusive dates)

Final Report - 1 May 1968 to 30 April 1969

5. AUTHOR(S) (Last name, first name, initial)

Kistler, Charles W., Jr., and Niesz, Dale E.

6. REPORT DATE

9 June 1969

7a. TOTAL NO. OF PAGES

58

7b. NO. OF REFS

12

8a. CONTRACT OR GRANT NO.

N00019-68-C-0176

b. PROJECT NO.

c.

d.

9a. ORIGINATOR'S REPORT NUMBER(S)

THIS DOCUMENT IS SUBJECT TO SPECIAL EXPORT CONTROLS AND EACH TRANSMITTAL TO FOREIGN GOVERNMENTS OR FOREIGN NATIONALS MAY BE MADE ONLY WITH [redacted] COMMANDER, NAVAL AIR SYSTEMS COMMAND, AIR_____, WASHINGTON, D.C. 20360

10. AVAILABILITY/LIMITATION NOTICES

Qualified Requesters may obtain copies of this report direct from the Defense Documentation Center, Cameron Station, Alexandria, Virginia. [redacted]

11. SUPPLEMENTARY NOTES

Includes data from Quarterly Progress Letter Reports Nos. 1-3.

12. SPONSORING MILITARY ACTIVITY

U. S. Naval Air Systems Command
Department of the Navy

13. ABSTRACT

An investigation was conducted to develop and evaluate carbon filament reinforced nickel.

Dense nickel-matrix composites were fabricated by precompacting and hot isostatically pressing aligned bundles of filaments to which the nickel matrix had been applied as uniform coatings on the individual filaments by electroless deposition. The specimens had uniform microstructures, essentially continuous filaments, and a relatively high-purity phosphorus-free matrix. A significant increase in filament breakage and decrease in composite density were noted when uniaxial rather than radial compaction was used during final densification. Porosity formation and associated microstructural degradation was shown to be dependent on oxygen, nitrogen, and hydrogen impurities in the composite. A vacuum annealing treatment was developed which reduced these impurities to a point where microstructural degradation during high-temperature annealing was insignificant. Removal of these impurities also substantially reduced internal oxidation caused by porosity formation.

The room-temperature tensile strength parallel with the filament orientation was 79,000, 97,000, and 86,000 psi for filament loadings of 43, 49, and 57 volume percent, respectively. Annealing for 100 hours at temperatures up to 2200 F did not reduce the room temperature strength significantly. However, thermal cycling did produce a significant strength reduction. After 100 cycles to 1800 F, the strength was 58,000 psi, but this strength reduction may be a strong function of the oxygen partial pressure in the atmosphere surrounding the specimen. The strength measured at elevated temperatures decreased more rapidly with temperature than predicted by the simple rule of mixtures. At 2000 F, the measured strength was 36,000 psi.

Possible reasons for the low measured strengths at elevated temperatures are discussed. The reasons for the low strengths (and moduli) measured at room temperature are discussed, and the possible mechanism for strength reduction due to thermal cycling are reviewed.

DD FORM 1 JAN 64 1473

Unclassified

Security Classification

Unclassified

Security Classification

14. KEY WORDS	LINK A ROLE	LINK A WT	LINK B ROLE	LINK B WT	LINK C ROLE	LINK C WT
Filament-Reinforced Metals						
Nickel						
Carbon Filaments						
Electroless Deposition						
Hot Isostatic Pressing						
Swaging						
Compatibility						
Oxidation Resistance						
Tensile Strength						
Stress-Strain Behavior						
Elastic Moduli						

Unclassified

Security Classification